



Universitetet
i Stavanger

FACULTY OF SCIENCE AND TECHNOLOGY

MASTER'S THESIS

Study program/specialization: MSc Petroleum Engineering / MSc in Well Engineering	The Spring semester, 2022 Open
Authors: Muhammad Usman and Jahanzaib Mazhar	<i>Muhammad Usman Jahanzaib</i> (signature of authors)
Supervisor(s): Dr. Alf Kristian Gjerstad	
Title of master's thesis: Analyze Gelling Properties for Time-Dependent Non-Newtonian Fluids Credits: 60	
Keywords:	Number of pages: 83
Gelling Properties Thixotropy Gel Strength Maximum Overshoot Stress	+ supplemental material/other: Stavanger, 15.06.2022
Title page for Master's Thesis Faculty of Science and Technology	

- MASTER THESIS -

Analyze Gelling Properties for Time-Dependent Non-Newtonian Fluids

Written by:

**Muhammad Usman and
Jahanzaib Mazhar**

Supervised by:

Dr. Alf Kristian Gjerstad



Faculty of Science and Technology
Department of Petroleum Engineering
Spring, 2022

ABSTRACT

Drilling fluids are visco-elastic materials. This means that they behave as a viscous fluid when subject to sufficient shear stress and like an elastic solid when they are in near static conditions. Both properties are time-dependent.

While drilling a well, there could be many instances when a change in the velocity of drilling fluid is required. For instance, we may have to adjust the pump flow rate depending upon the formation drilled. In a similar manner, there could be variations in the flow rate due to the movement of the drill string as it can move axially, rotationally, and side-wise. Another example is the change of flow rate owing to the difference in the flow geometry while passing from the annulus. In all these cases, the drilling fluid required a definite time to attain new equilibrium conditions.

Nevertheless, the time-dependence rheological properties of drilling fluids are usually not measured during drilling operations. Additionally, in the lab measurements, seldom are experiments performed beyond 30 minutes of resting time. Consequently, it is difficult to estimate how thixotropy impacts pressure losses in drilling operations. Against this backdrop, our research is focused on the analysis of the gelling properties of time-dependent non-Newtonian fluids.

We have systematically measured the time-dependence of the rheological properties of different samples of water-based and oil-based fluids with a scientific rheometer in order to capture how the gel strength of the drilling fluids responds to variations of other relevant parameters involved. Furthermore, we have analyzed the behaviours of those fluids for the longer resting times until no further gel strength is developed in them.

Key Words: Thixotropy, Gelling Properties, Time-dependent Non-Newtonian Fluids

ACKNOWLEDGMENTS

This thesis is written and submitted as a fulfilment of the requirements for the MSc degree in Petroleum Engineering at the University of Stavanger (UiS), Norway. The work has been carried out in a period between 17th January and 15th June.

We want to take this opportunity to express our sincere gratitude to our supervisor Dr Alf Kristian Gjerstad for his support, trust, motivation, guidance, and encouraging us throughout the thesis. He was always available to us for supervision and prompt feedback despite his busy schedule.

Secondly, we would like to extend our gratitude to Kim Andre Nesse Vorland whose support, assistance, collaboration, analysis, and comments helped us in maturing our work.

Thirdly, we would like to appreciate Halliburton and Baker Hughes for providing us with the drilling muds to execute the laboratory tests.

Fourthly, we would like to express our appreciation to the University of Stavanger for allowing us to use the labs, providing us with drilling fluid materials, and for offering an amazing study atmosphere during our Master's degree.

Lastly, we would like to thank our parents, family, and friends for their constant prayers and support during this journey.

Muhammad Usman
Jahanzaib Mazhar
15.06.2022

Nomenclature

WBM: water-based mud

OBM: oil-based mud

τ : shear stress [lbs/100ft²]

γ : shear rate [sec⁻¹]

μ : viscosity [Nsecm⁻²]

n : flow behavior index

S : gel strength at any time t

S' : ultimate gel strength

Table of Contents

Nomenclature	V
Chapter 1: Introduction	1
1.1 Background.....	1
1.2 Purpose.....	1
1.3 Approach.....	2
1.4 Limitations	2
1.5 Structure of the thesis.....	3
Chapter 2: Theory and Literature Review	4
2.1 Functions of Drilling Fluids.....	4
2.2 Basic Principles of Rheology.....	4
2.2.1 Shear Stress.....	5
2.2.2 Shear Rate	5
2.2.3 Viscosity	6
2.2.4 Yield Point (YP)	7
2.2.5 Gel Strength	8
2.2.6 Thixotropy.....	9
2.3 Rheopexy	10
2.4 Rheological Modelling.....	11
2.4.1 Newtonian Model	11
2.4.2 Bingham Plastic (BP) Model.....	12
2.4.3 Power Law (PL) Model	12
2.4.4 Herschel and Bulkley (HB) Model	13
2.5 Applicability of Models in Drilling Fluid Domain	13
2.6 Types of Drilling Fluids.....	14
2.6.1 Water-Based Muds (WBM).....	14
2.6.2 Oil-Based Muds (OBM).....	15
2.7 An Account of Previous Works on Thixotropy	17
Chapter 3: Methodology	20
3.1 Drilling Muds Used in Experiments	20

3.1.1	Water-Based Mud 1 (WBM 1).....	20
3.1.2	Water-Based Mud 2 (WBM 2).....	22
3.1.3	Oil Based Mud (OBM)	24
3.2	Field Procedure of Gel Strength Measurement.....	26
3.3	Experimental Setup.....	26
3.3.1	Specification of the Rheometer	27
3.3.2	Sample Loading Systems.....	28
3.4	Experimental Procedure.....	31
3.4.1	Preliminary Steps	31
3.4.2	Measuring Steps.....	32
Chapter 4:	Selection of Parameters.....	33
4.1	Homogeneity Conformity	33
4.2	Initial Shear Rate Time Testing	34
4.3	Local Temperature Effects.....	38
4.4	Linear Acceleration Testing.....	42
4.4.1	Maximum Stress Overshoot vs. Resting Time.....	43
4.4.2	Testing at Extremely Low Shear Rate Value.....	46
4.5	Conclusion	47
Chapter 5:	Experimental Results and Discussion	48
5.1	WBM 1.....	48
5.2	WBM 2.....	51
5.2.1	Case Scenarios.....	51
5.2.2	Case A.....	51
5.2.3	Case B.....	53
5.2.4	Case C.....	55
5.3	ENVIROMUL OBM	58
5.3.1	Case Scenarios.....	58
5.3.2	Case A.....	59
5.3.3	Case B.....	61
5.3.4	Case C.....	63
5.4	Further Work Recommendations	66
References	67

This page is intentionally left blank

List of Figures

<u>Figure 2.1 Illustration of friction between the fluid and moving plate</u>	5
<u>Figure 2.2 Showing the relationship between effective viscosity and increasing shear rate</u> ..	7
<u>Figure 2.3 Yield Point as extrapolation of yield stress</u>	7
<u>Figure 2.4 Thixotropic behavior</u>	10
<u>Figure 2.5 Comparison of Rheological Models on Stress vs Strain Plot</u>	11
<u>Figure 2.6 Pseudo plastic behavior of a drilling fluid</u>	13
<u>Figure 3.1 A 5-liter container of KCl Polymer WBM 1</u>	20
<u>Figure 3.2 After mixing KCl Polymer WBM 1 and dividing into 6 bottles for storage</u>	21
<u>Figure 3.3 A 1-liter bottle of KCl Polymer WBM 2</u>	22
<u>Figure 3.4 Heidoph Rotary equipment for mixing of KCl Polymer WBM 2</u>	23
<u>Figure 3.5 Type of stirrer to be used with Heidoph rotary equipment</u>	23
<u>Figure 3.6 A 5-liter container of Enviromul OBM</u>	25
<u>Figure 3.7 After mixing Enviromul OBM and divided into 6 bottles for storage</u>	26
<u>Figure 3.8 Anton Paar Modular Compact Rheometer (MCR) 302</u>	27
<u>Figure 3.9 Setup showing the air supply equipment to Anton Paar MCR 302</u>	28
<u>Figure 3.10 Illustration of cocentric cylinder system</u>	29

<u>Figure 3.11 Illustration of Plate-Plate system</u>	29
<u>Figure 3.12 Illustration of Cone-Plate System</u>	30
<u>Figure 3.13 Illustration of Double Gap system</u>	31
<u>Figure 3.14 Control Panel of MCR 302 Software</u>	32
<u>Figure 4.1 Stress overshoots resembling homogeneous response from different samples</u> ...	34
<u>Figure 4.2 Stress overshoots following different initial shear rates (increasing order)</u>	35
<u>Figure 4.3 Stress overshoots following different initial shear rates (decreasing order)</u>	37
<u>Figure 4.4 Comparison of initial shear rate variation with respect to time</u>	38
<u>Figure 4.5 Comparison of Stress overshoots of 2 minutes applied initial shear rate indicating local temperature effect</u>	40
<u>Figure 4.6 Comparison of Stress overshoots of 5 minutes applied initial shear rate indicating local temperature effect</u>	41
<u>Figure 4.7 Stress overshoots following shear rate increment from 0 to 0.5 per second</u>	44
<u>Figure 4.8 Stress overshoots following shear rate increment from 0 to 2 per second</u>	45
<u>Figure 4.9 Stress overshoots following shear rate increment from 0 to 5.1 per second</u>	47
<u>Figure 4.10 Comparison of stress overshoots following different shear rate increments</u>	48
<u>Figure 5.1 Stress overshoots in the WBM 1 following different resting times</u>	51
<u>Figure 5.2 Maximum Stress overshoots in the WBM 1 as logarithmic function following different resting times</u>	52

Figure 5.3 Stress overshoots in the WBM 2 during 0 to 2 per second initial rate for 0.5 seconds following different resting times 55

Figure 5.4 Maximum Stress overshoots in the WBM 2 as logarithmic function during 0 to 2 initial shear rate for 0.5 seconds following different resting times 56

Figure 5.5 Stress overshoots in the WBM 2 during 0 to 5.1 per second initial rate for 0.5 seconds following different resting times 57

Figure 5.6 Maximum Stress overshoots in the WBM 2 as logarithmic function during 0 to 5.1 initial shear rate for 0.5 seconds following different resting times 58

Figure 5.7 Stress overshoots in the WBM 2 during 0 to 5.1 per second initial rate for 1.25 seconds following different resting times 59

Figure 5.8 Maximum Stress overshoots in the WBM 2 as logarithmic function during 0 to 5.1 initial shear rate for 1.25 seconds following different resting times 60

Figure 5.9 Comparison of case scenarios for WBM 2 following different resting times 61

Figure 5.10 Stress overshoots in the Enviromul OBM during 0 to 2 per second initial rate for 0.25 seconds following different resting times 63

Figure 5.11 Maximum Stress overshoots in the Enviromul OBM as logarithmic function during 0 to 2 initial shear rate for 0.25 seconds following different resting times 64

Figure 5.12 Stress overshoots in the Enviromul OBM during 0 to 5.1 per second initial rate for 0.25 seconds following different resting time 65

Figure 5.13 Maximum Stress overshoots in the Enviromul OBM as logarithmic function during 0 to 5.1 initial shear rate for 0.25 seconds following different resting times 66

Figure 5.14 Stress overshoots in the Enviromul OBM during 0 to 5.1 per second initial rate for 0.625 seconds following different resting times 67

Figure 5.15 Maximum Stress overshoots in the Enviromul OBM as logarithmic function during 0 to 5.1 initial shear rate for 0.625 seconds following different resting times 68

Figure 5.16 Comparison of case scenarios for Enviromul OBM following different resting times 69

List of Tables

<u>Table 3.1 Contents of KCl Polymer WBM 2</u>	22
<u>Table 3.2 Contents of Enviromul OBM</u>	24
<u>Table 3.3 Pros and cons of cocentric cylinder system</u>	29
<u>Table 3.4 Pros and cons of plate-plate system</u>	30
<u>Table 3.5 Pros and cons of cone-plate system</u>	30
<u>Table 3.6 Pros and cons of double gap system</u>	31
<u>Table 4.1 Homogeneity conformity testing summary</u>	33
<u>Table 4.2 Initial Shear Rate testing summary in ascending order</u>	35
<u>Table 4.3 Initial Shear Rate testing summary in descending order</u>	36
<u>Table 4.4 Comparison of initial shear rate variation with respect to time</u>	38
<u>Table 4.5 Local Temperature Effect testing Summary with 2 minutes applied initial shear rate</u>	39
<u>Table 4.6 Comparison of Stress overshoots of 2 minutes applied initial shear rate indicating local temperature effect</u>	39
<u>Table 4.7 Local Temperature Effect testing Summary with 5 minutes applied initial shear rate</u>	40
<u>Table 4.8 Comparison of Stress overshoots of 5 minutes applied initial shear rate indicating local temperature effect</u>	4

<u>Table 4.9 Shear rate increment from 0 to 0.5 per second testing summary</u>	44
<u>Table 4.10 Shear rate increment from 0 to 2 per second testing summary</u>	45
<u>Table 4.11 Shear rate increment from 0 to 5.1 per second testing summary</u>	46
<u>Table 4.12 Extremely low shear rate testing summary</u>	48
<u>Table 5.1 Stress overshoots in the WBM 1 following different resting times</u>	50
<u>Table 5.2 Stress overshoots in the WBM 2 during 0 to 2 per second initial rate for 0.5 seconds following different resting times</u>	54
<u>Table 5.3 Stress overshoots in the WBM 2 during 0 to 5.1 per second initial rate for 0.5 seconds following different resting times</u>	57
<u>Table 5.4 Stress overshoots in the WBM 2 during 0 to 5.1 per second initial rate for 1.25 seconds following different resting times</u>	58
<u>Table 5.5 Stress overshoots in the Enviromul OBM during 0 to 2 per second initial rate for 0.25 seconds following different resting times</u>	62
<u>Table 5.6 Stress overshoots in the Enviromul OBM during 0 to 5.1 per second initial rate for 0.25 seconds following different resting times</u>	64
<u>Table 5.7 Stress overshoots in the Enviromul OBM during 0 to 5.1 per second initial rate for 0.625 seconds following different resting times</u>	66

Chapter 1: Introduction

1.1 Background

Drilling mud is an inevitable part of well drilling process. It has a range of functions varying from providing lubrication, cutting transportation and suspension, to avoiding catastrophic incidents such as kick control. Therefore, it is important to optimize drilling fluid parameters.

One of the important functions is to transport the cuttings effectively during circulation and suspend cuttings while in a stationary or near stationary state. It means that drilling fluid is a part of the system that keeps on changing between a dynamic and a steady-state condition. In other words, we want the drilling fluid to be in a gel-like state to suspend the cuttings, and during pump flow, it should be less viscous but should maintain integrity to transport the cuttings. The value of gel strength keeps on increasing during the resting state. However, we do not want it to increase beyond a certain point as when we resume the circulation, this gel strength must be broken to start the fluid flow. The higher pump pressure required to break the gel strength may fracture the formation as well.

The field procedure normally measures gel strength in terms of deflection of the Fann 35 viscometer after a certain resting time. Likewise, in literature, it is not common to analyze the gelling properties beyond 30 minutes.

Set in this context, it is important to analyze the gelling properties of drilling fluid thoroughly. An improved understanding of gel evolution could lead to a better and improved mud design, calibrating existing thixotropic models, building new models, maintaining accurate pump pressure, and avoiding any unwanted and unplanned incidents.

1.2 Purpose

The main objective of this work is to acquire a better understanding of the thixotropic nature of drilling muds by measuring the build-up of gel strength on a scientific rheometer. While it is rare to find data in the literature that treats gelling times above 30 minutes, we show that after 30 minutes, the gelling process continues. This is important for field practices where flow circulation could be stopped for numerous hours. In addition, the effect of various other

parameters such as initial shear rate time, local temperature effect, and acceleration of linear shear rates is measured.

1.3 Approach

The objectives of this thesis work have been obtained by using the following approach.

Firstly, we reviewed the theory to understand and strengthen the concepts related to rheology. Building on that, we analyzed the work done by the other authors on thixotropy and gelling properties.

Secondly, an in-depth experimental approach using Anton Paar Rheometer MCR 302 was employed to analyze the parameters and the extent to which they contribute to the gel strength. In this work, gel strength is measured in terms of maximum stress overshoot during the start-up of the flow.

Thirdly, we performed experiments on three different muds and jotted down the results and findings. In the end, a comprehensive summary of each mud and future work recommendations are also presented.

1.4 Limitations

The experimental work performed in this thesis has certain limitations. By changing these limiting factors, the results could vary.

One, cocentric cylindrical geometry (discussed in section 3.3.2.1) is used in Rheometer to determine the value of gel strength in terms of the maximum value of stress overshoot.

Second, the experiments have been performed at 20 degrees centigrade.

Finally, the normal force has to be calibrated to 0.00 N before the start of the experiment so that the results will not be affected by the force acting upon the plate.

1.5 Structure of the thesis

From this point forward, the dissertation is organized in the following way:

- In Chapter 2, relevant theory and literature review are presented
- In Chapter 3, descriptions of drilling muds used, sampling mechanism, and a brief overview of the experimental methodology are given
- In Chapter 4, the experimental details and results are presented to gauge the extent of various parameters affecting gel strength
- In Chapter 5, experiments performed on three different muds, their results, and discussion is rendered. Furthermore, a comprehensive discussion and future work recommendations are also listed.

Chapter 2: Theory and Literature Review

This chapter contains theoretical background, definition and description of some key terms relevant to the experiments performed in the masters. An overview of drilling fluids, their rheological properties, and relevant models to study their behaviors is presented. Later in the chapter, the literature review relevant to gelling properties is presented.

2.1 Functions of Drilling Fluids

The drilling operation of a well relies heavily on the quality of drilling fluids. Although there are many functions of drilling mud, the primary function is to remove the cuttings efficiently. The other main functions of drilling are [1,2,3].

- Controlling bottom hole pressure and avoiding the inflow of unwanted formation fluids
- Suspending the solids and weighting materials during rotary and static conditions
- Providing mechanical and chemical stability to the openhole sections of the wellbore
- To reduce the flow of mud into formation, building low-permeable filter cake in the wellbore
- Reduction in the friction between the drill pipe and wellbore wall by providing lubrication
- Cooling down the drillstring and drill bit
- Ensure maximum information from the well
- Support partial weight of drill string or casing

To achieve these, the drilling fluids are pumped through the drill pipe, discharged through the drill bit, and returned to the surface through the annulus between drill string and formation. Before going into further details of the types of drilling fluid (discussed in section 2.6), it is vital to understand the rheology of drilling fluids thoroughly.

2.2 Basic Principles of Rheology

Rheology is defined as the science of deformation and flow of matter. Especially since the advent of the 20th century, it has become a multidisciplinary subject and experts from a range of industries are working in their relevant fields for an enhanced understanding about applied rheology (Mezger, 2011). It also describes the flow pattern of fluids i.e., laminar, transient or turbulent nature of flow.

During flow, there are different layers of a fluid that move at varying velocities. This implies that molecules are moving relative to one another when the fluid is in motion. In a system that consists of two plates with fluid flowing in between the plates where one plate is moving in one direction while the other is stationary, the fluid will shear because of the friction between the fluid and the moving plate [3]. Figure 2.1 [4] illustrates how the plate with velocity causes the fluid to shear.

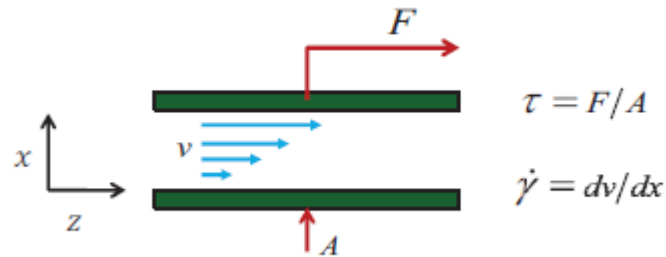


Figure 2.1 Showing the friction between the fluid and moving plate

2.2.1 Shear Stress

Shear stress is the force applied per unit area of the fluid. When the force is applied, deformation is produced and mathematically defined as

$$\tau = F/A \quad (2.1)$$

where F is a force acting on one of the boundary surfaces, and A is the area of the surface. Shear stress has typically a unit of lbs/100ft².

2.2.2 Shear Rate

Shear rate is the velocity gradient of a fluid. It is the rate at which the shear is applied. The shear rate is defined as,

$$\gamma = \frac{dv}{dx} \quad (2.2)$$

Or it can be written as

$$\gamma = \frac{\text{Velocity difference}}{\text{distance}}$$

It has typical units of sec⁻¹.

The fluids will behave differently when undergoing the same shear rate depending upon the conditions which the fluid has previously experienced. This means the fluid depicts time-dependent behaviour which complicates the understanding of the rheology of fluids.

2.2.3 Viscosity

Viscosity is the measure of a fluid's resistance to deform when undergoing stress. It describes the thickness of a fluid which means larger internal friction, and hence resistance to flow. The viscosity of fluids varies depending upon the structure of the fluid and the flow pattern. Viscosity is a static property of a fluid.

Mathematically, it can be written as

$$\mu = \frac{\tau}{\dot{\gamma}} \quad (2.3)$$

Where,

τ = Shear stress

$\dot{\gamma}$ = Shear Rate

μ = Viscosity

It has a typical unit of Pa-sec ($\text{Nm}^{-2}\cdot\text{sec}$).

2.2.3.1 Effective Viscosity

To predict the behavior of a fluid and determine its properties correctly, it is important to have a thorough knowledge of how fluids change under different conditions. Viscosity is a property that varies with several external factors. For example, effective viscosity is the viscosity affected by various variables such as shear rate (discussed in section 2.2.2), temperature, pressure, time of sharing and chemical or physical nature of the fluid [3]. The effective viscosity of a fluid decreases with increasing shear rates as illustrated in the figure 2.2 [5]. Effective viscosity is also called apparent viscosity. This effect is also known as shear thinning effect. As a matter of fact, during mud circulation, it is this shear thinning effect which reduces circulating pressure and pressure losses.

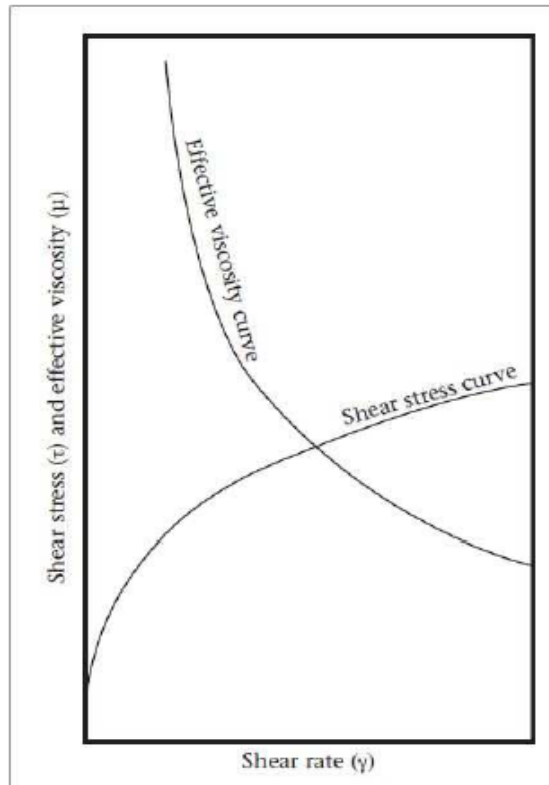


Figure 2.2 Showing the relationship between effective viscosity and increasing shear rate

2.2.4 Yield Point (YP)

The yield point is the yield stress extrapolated to a shear rate of zero, and plastic viscosity is the slope of the curve as shown in figure 2.3 [5]. In short, it is the resistance of the initial flow of fluid or the stress required in order to start the fluid flow. The yield point, like viscosity, is a static property of a fluid.

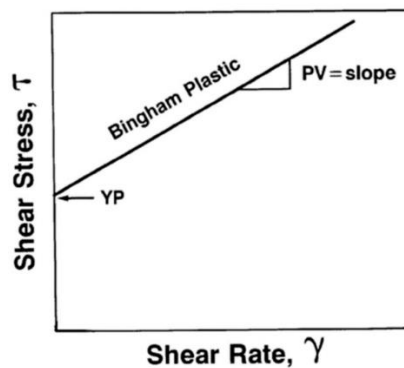


Figure 2.3 Yield Point as extrapolation of yield stress

In the oil and gas industry, the yield stress of the drilling fluid is one of the crucial factors for the evaluation of barite sag, hole cleaning, ECD, swab/surge pressure, and other issues

pertaining to drilling fluids [6]. YP is used to evaluate the ability of mud to lift cuttings out of the annulus as well. A high YP implies a non-Newtonian fluid, one that carries cuttings better than a fluid of similar density but lower YP. Just like viscosity, yield stress is also time-dependent. It implies that yield stress measurement depends on fluid previous history and condition i.e., static or sheared. In this backdrop, the yield point should be at a reasonable value for hydraulics and cutting transport performance [7,8].

Yield point can be estimated by using rheological models that will be discussed in section 2.4.

2.2.5 Gel Strength

The gel strength is the shear stress of drilling mud that is measured at low shear rate after the drilling mud is static for a certain period of time. To put in another words, gel strength is the measure of interparticle forces in drilling fluid and indicates the amount of gelling that will occur when circulation is stalled. The right gel strength prevents cuttings from settling in the borehole. Unlike YP and Viscosity, yield point is a dynamic property of a fluid.

According to the API standard, the gel strength is defined as the shear stress measured (*using Fann viscometer*) at the shear rate of 3 rpm after the drilling mud has been at rest for 10 sec, 10 min, and 30 min. The dial readings can then be directly reported in *lb/100ft²* as the gel strength of the mud at the mentioned time intervals [3,10].

2.2.5.1 Importance of Gel Strength in Drilling Fluids

Drilling fluid performance is a key contributor to the success of a drilling operation. Gel strength is a property of drilling fluid that impacts its performance greatly. To lift the cuttings, mud pump management comes into play. In this regard, special care has to be taken to avoid fracturing the formation and loss of circulation owing to excessive pump pressure

When the gel strength is too high, the drilling fluid tends towards solidification in static conditions. This is dangerous because it may require a very high pump pressure to get the drilling fluid moving again. High pressures could cause a frac-out leading to leaked drilling fluid into the ground [5,10].

When the gel strength is too low, cuttings tend to drop out of the drilling fluid too easily. Drilling fluid is designed to hold cuttings in suspension. If this fails, cuttings build up on the lower side of the bore and eventually could cause a blockage. It can also result in a stuck pipe. Similarly, barite could start settling down as well. This is a hazardous situation because releasing the pipe could damage the bore and the equipment [10,11].

Having said this, drilling fluid properties play a critical role in the success of a horizontal directional drilling or vertical drilling project. Gel strength is the specific property related to how easily the drilling fluid will hold cuttings in suspension and how strong the gel state becomes when the fluid stops flowing. The right balance must be struck for the specific formation conditions to prevent costly repairs and downtime due to blockages or fracking-outs. These properties can be controlled in a mud system by chemical treatment [9,10,11].

2.2.5.2 Gel Strength Consideration in Horizontal and Vertical Drilling

Horizontal and vertical drilling applications are quite different when it comes to the best gel strength to use. Vertical drilling is a simpler process requiring the mud circuit to overcome the forces of gravity to pump out drilling fluid with cuttings from the well. If the flow rate is stopped for any reason, cuttings held in suspension have a long way to fall down the well before accumulating at the bottom. An optimized gel strength will therefore be sufficient to slow down this effect of gravity and prevent blockages or pressure problems.

On the other hand, horizontal directional drilling is much more susceptible to blockages caused by a buildup of cuttings. If the flow in the mud circuit is shut off, the suspended cuttings only have to drop a few inches before building up on the lower surface of the bore. A high gel strength is very important to keep the cuttings suspended even if the mud circuit stops flowing for a short time.

2.2.6 Thixotropy

H. A. Barnes defines thixotropy as “the temporal rheological response of a microstructure to changes in imposed stress or strain rate” [27]. To put it in other words, thixotropy is a history and time-dependent behavior of drilling fluids. This time-dependent behavior complicates the understanding of the behaviour of the fluid. It implies that the fluid will behave differently

under the same shear rate, depending on the shear rate the regime fluid previously has experienced.

Most drilling fluids are thixotropic fluids. When drilling a well this means that during low shear rates, or at quiescence, the viscosity is higher, and has a higher ability to keep heavy particles suspended. When the drilling fluid is pumped at a high shear rate, the viscosity decreases so that the drilling fluid flows easier and there is no need for high viscosity because the velocity of the drilling fluid transports the heavy particles. This change between becoming a semi-rigid and fluid state is reversible [3]. The thixotropic behavior is shown in figure 2.4 [2].

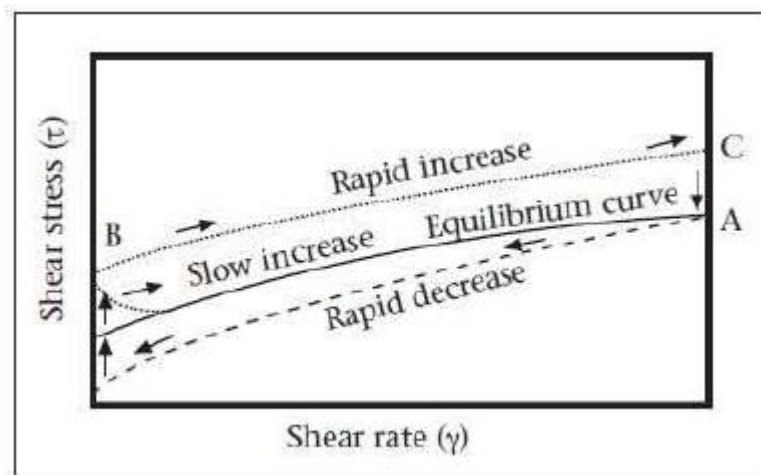


Figure 2.4 Thixotropic behavior (MI SWACO, 2006)

In the figure shown above, the equilibrium curve is the solid line. In case of thixotropic fluid, there are three possible scenarios Firstly, if the flow is slowly reduced to zero, the gel solidification will follow the equilibrium curve from A to B. Secondly, if the flow rate is reduced suddenly, then the gel solidification will follow the dashed curve named “Rapid decrease”. Thirdly, if the flow rate is increased suddenly, the thixotropic fluid will behave as per the top curve, the dotted line from B to C.

2.3 Rheopexy

Rheopexy is related to shear thickening, contrary to shear thinning. This means that fluid viscosity increases when exposed to shear stress over time. Normally, drilling fluids do not exhibit rheopexy.

2.4 Rheological Modelling

Rheological modelling is a mathematical way to describe the rheology of a drilling fluid. To achieve this, experiments are performed to determine the empirical constants. A rheometer is one of the commonly used apparatus in the experiments. In rheometers, various geometries such as a coquette, parallel late or cone and plate geometry are used. The data obtained from these experiments is plotted (shear stress vs. shear rate) to generate a flow curve. The flow curve is then compared against the shape of the predefined different rheological models to estimate which rheological model best resembles the fluid on which the experiment has been performed.

Figure 2.5 shows a plot with the most commonly used rheological models [12].

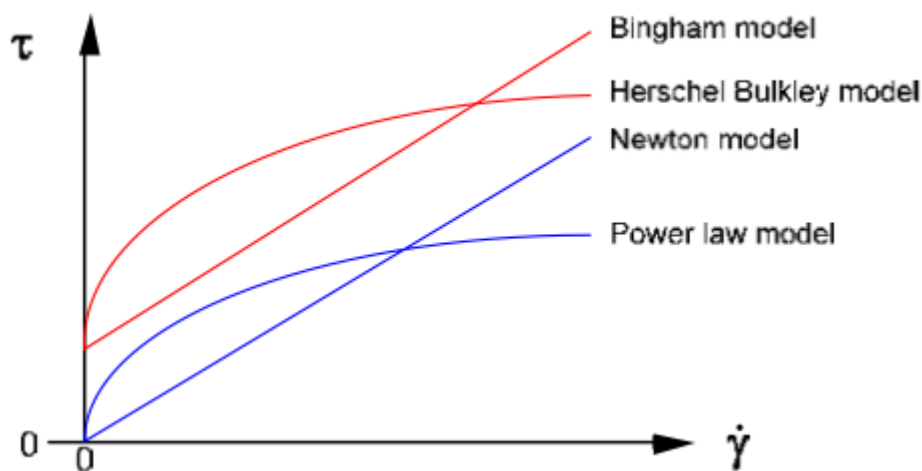


Figure 2.5 Comparison of Rheological Models on Stress vs Strain Plot

2.4.1 Newtonian Model

For a Newtonian fluid, at constant temperature, the shear stress and shear rate are directly proportional. The proportionality index is the viscosity. Mathematically, the relationship between shear stress and shear rate is given by [1,3,12]

$$\tau = \mu * \dot{\gamma} \quad (2.4)$$

where,

τ = shear stress

μ = viscosity

γ = shear rate

2.4.2 Bingham Plastic (BP) Model

In the early 1900s, E.C. Bingham first recognized that some fluids exhibited a plastic behavior, distinguished from Newtonian fluids, in that they require yield stress to initiate flow [12]. No bulk movement of the fluid occurs until the applied force exceeds the yield stress. The yield stress is commonly referred to as the Yield Point.

The shear stress and shear rate relationship for the Bingham Plastic Model is given by [1,3,12]:

$$\tau = \tau_o + \mu_{pl} * \gamma \quad (2.5)$$

where,

τ = shear stress

τ_o = yield point

μ_{pl} = Plastic viscosity

γ = shear rate.

2.4.3 Power Law (PL) Model

Power law models best represent the relationship between shear stress and shear strain for pseudo plastic fluids. Mathematically it is given by [1,3,12];

$$\tau = K \gamma^n \quad (2.6)$$

where,

τ = shear stress

K = consistency factor

γ = shear rate

n = flow behavior index

2.4.4 Herschel and Bulkley (HB) Model

By adding yield stress parameter in power law model, Herschel and Bulkley model is achieved. In mathematical format, it is written as [1,3,12]

$$\tau = \tau_0 + K \dot{\gamma}^n \quad (2.7)$$

2.5 Applicability of Models in Drilling Fluid Domain

The behaviour of most of the drilling fluid is between the behaviours described by the Newtonian Model and the Bingham Plastic Model [3] as shown in figure 2.6. This behaviour is called pseudo plastic.

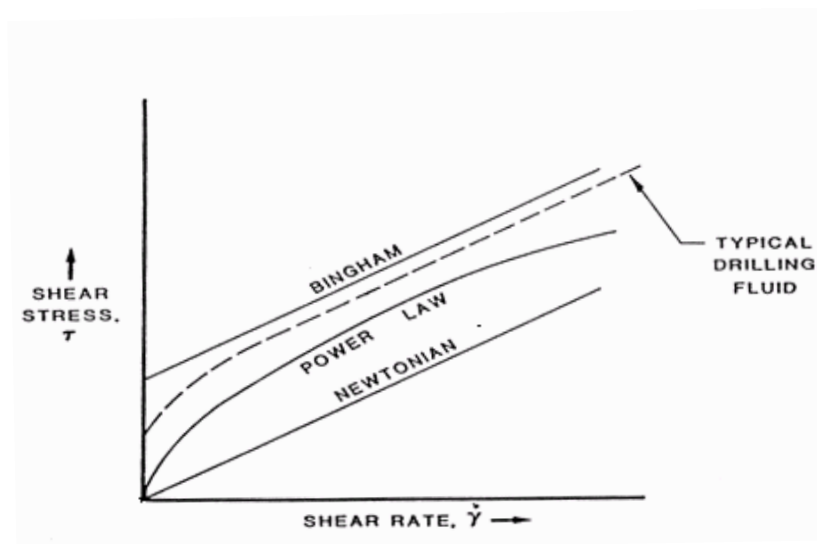


Figure 2.6 Pseudo plastic behavior of a drilling fluid

A typical drilling fluid exhibits yield stress and is shear thinning. At high rates of shear, all models represent a typical drilling fluid reasonably well. Differences between the models are most pronounced at low rates of shear, typically the shear rate range is most critical for hole cleaning and the suspension of weight material [3]. As a consequence, HB model is more commonly used in the drilling industry as compared to the other simpler models such as PL and BP models [3].

2.6 Types of Drilling Fluids

Drilling fluid is a complex fluid having specific properties to drill the well safely and achieve other objectives (discussed in section 2.1). It consists of a based fluid. In that base fluid, various substances and chemicals are added to achieve the required rheological properties. Mainly, there are two categories of drilling muds. One is water-based muds (WBM), and the second is oil-based muds (OBMs). The basic theory of both muds is discussed in the following section, and both muds have been used in experiments performed to cover the topic from multiple areas. The details of the specific muds used in the experiments can be found in section 3.1.

2.6.1 Water-Based Muds (WBM)

In WBM, salt water or fresh water is the base fluid in which bentonite and polymers are added to increase the viscosity and gel strength [3,14].

Advantages

- Low cost
- Less impact on the environment
- Easy to handle
- Higher capability to suspend the solids due to its higher gel strength

Disadvantages

- Reaction with shale
- Not very suitable for higher temperature wells

2.6.1.1 Key Components of WBM

The following are the major constituents of a WBM.

2.6.1.1.1 Bentonite

It provides the required viscosity and helps in lift particle suspending capabilities, that is gel strength [14]. It is not a weighing material and does not increase the fluid density. Due to its availability in large quantities, low cost and little contribution towards pollution, it has been used for drilling the top sections of wells. However, while going deeper into the well, more and more bentonite would be required. In turn, large storage space on offshore platforms and high transportation costs would accrue. Therefore, a better alternative to bentonite is the addition of polymers [16].

2.6.1.1.2 Polymer

The history of adding polymers in WBM is very old. Although they are more expensive than bentonite, the same objective could be achieved by adding a smaller volume of polymers compared to bentonite [15]. Carboxymethylcellulose (CMC), Poly Anionic Cellulose (PAC) polymer and Xanthan Campestris (Xanthan-XC) biopolymer are among the most commonly used polymers to provide drilling mud system with viscosity, filtration control, and gel strength [3,14,15].

2.6.1.1.3 Barite

It is the most commonly used weighting material in drilling fluids. Primarily, its low cost, high specific density, and inability to react with other substances make it the best candidate to achieve the desired objectives. Chemically, barium sulfate (BaSO_4) is a major part of it. However, it also contains BaSO_3 and other heavy minerals [15,16].

2.6.2 Oil-Based Muds (OBM)

In OBM, synthetic oil is the main component. In this oil, water is added to make an invert emulsion.

Advantages

- Reduces friction between the wellbore and drillstring
- Shale stability and inhibition
- Temperature stability
- Resistance to chemical contamination
- Reduced production damage
- Reduced tendency for differential sticking
- Drilling underbalanced
- Higher rate of penetration
- Reduced corrosion

Disadvantages

- High initial cost
- Mechanical shearing is required
- Environmental considerations

- Reduced kick detection ability
- Barite sag and difficulty in hole cleaning
- High cost of lost circulation
- Disposal problems
- Rig cleanliness and hazardous vapors
- Fire hazard
- Special logging tools requirement
- Aqueous contamination

2.6.2.1 *Emulsion*

The system in which both continuous and dispersed phases are liquid is called an emulsion. In the case of OBM, oil and water are continuous and dispersed phases respectively. It is important to maintain the stability of the emulsion. This can be achieved through either electrostatic stabilization or by adding some other particles such as clay.

2.6.2.2 *Flocculation*

When attractive forces between particles are larger than the repulsive forces, the particles will flocculate. If flocculation spreads on a large scale, the whole network will lead to gelling of the system [12].

2.6.2.3 *Sagging*

Barite sag occurs when heavy minerals in the barite and other solid particles, such as cuttings, fall into the bottom of the wellbore due to gravity. This phenomenon usually happens when circulation is stopped in vertical wells. On the other hand, in deviated and horizontal wells, it occurs due to a complex setting mechanism called “Boyocott settling.” According to this mechanism, heavier particles settle quickly at the low side of the wellbore, while the lighter fluids are at the high side. This makes barite sag a more complex issue in deviated wells as compared to vertical wells. At angles as high as 75°, significant barite sag was measured, and 60°-75° was the most critical range [17, 18]. The higher the amount of weighting material the higher the risk of occurring barite sag [18, 19].

Various problems and complications can arise due to sagging. For example, due to presence of heavy particles, mud in the deeper section will have high density which may fracture the formation. On the other hand, mud density will be lower in the shallower section owing to which there could be chances of well control incident. Consequently, barite sag could lead to both economic and safety-related issues during drilling operations [1].

To avoid these issues, mud with high gelling properties can significantly reduce barite sag. Nguyen et al (2011) showed that barite sag occurs 10 times faster in drilling fluid with a yield stress of 5 lb/100ft² compared to the same type of fluid with a yield stress of 12 lb/100ft² [17].

Owing to differences in chemical, physical, and rheological properties of both types of muds, barite sag is a severe problem in the case of OBM. The polymer structure in WBM helps in building gel whereas, in an invert-emulsion, the gel strength will not develop to the same extent as in WBMs [28].

2.7 An Account of Previous Works on Thixotropy

Although the rheology of drilling fluid is an area of intensive research, the experimental history pertaining to thixotropy dates back to 1935. The effect of thixotropy on the evaluation of the rheological parameter of drilling mud was first investigated by Jones and Babson [20]. They sheared the thixotropic muds at constant rates and observed the changes in torque with the passage of time. The torque values decreased sharply initially, then decreased gradually, and finally achieved equilibrium.

Another major step toward predicting long-term gel strengths was taken by Garrison (1939). He observed gelling rates of Californian bentonites and developed the following equation.

$$S = S'kt + kt \quad (2.8)$$

where

S is the gel strength at any time t

S' is the ultimate gel strength

k is the gel rate constant.

Eq. 2.8 may be written as

$$t_S = t_{S'} + 1S'k \quad (2.9)$$

The longest resting time to measure gel strength is up to one day reported by Weintritt and Hughes (1965) [20]. They measured the gel strengths of some field muds containing calcium sulfate and ferrochrome lignosulfonate in a rotary viscometer. For longer periods of resting time such as at two hours and thereafter, there was a deviation between their data and equation 2.8. Other than this, we are not aware about any literature where the equation was applied to the other types of muds which were not tested by Garrison.

H.A Barnes (1997) figured that it takes a minimum time before the drilling fluid achieves steady-state condition after the application of a certain shear rate. He pointed out that this is due to the reason that the drilling fluids are thixotropic i.e., their flow properties depend upon the history of shear rates applied.

Rommetveit et al (1997) studied the effects of temperature and pressure on deep wells and concluded that the rheology of drilling fluids significantly depends upon temperature and pressure [21]. While determining the drilling fluid rheology, it is common to assume constant temperature and pressure. The assumption holds true for shallow wells. However, in case of deep wells, where there is high pressure and high temperature (HPHT), and the difference between pore pressure (PP) and fracture gradient (FG) curves is small, this assumption can lead to serious problems such as unwanted flow of the formation fluids and well integrity problems. Furthermore, while studying the time dependent properties, they also figured that the gel strength increases by a good margin for high pressure and temperature.

Herzhaft et al. (2006) showed that a thixotropic model could explain yielding and thixotropy of drilling. Furthermore, the author proposed a method of fitting model parameters to oilfield viscometer [23]. Ragouilliaux et al. (2006) used the model proposed by Herzhaft et al (2006) to interpret creep tests and MRI velocimetry of a model oil-based drilling fluid.

Maxey (2007) used four model fluids to exhibit drilling fluid thixotropy. He subjected the fluids to sudden step changes in shear rate and measured the shear hysteresis while ramping the shear rate from low to high and high to low respectively [22].

Tehrani and Popplestone (2009) showed a thixotropic model to predict the effects of time and recent shear history on drilling fluid rheology [25].

Eric Cayeux and Amare Leulseged (2018) measured the time dependence rheological properties of various drilling fluids with a scientific calculator [25]. Furthermore, they modified an existing model to predict the shear stress as a function of shear rate while accommodating the shear history and gelling conditions. As claimed by the authors, the model fits better barring a few noticeable discrepancies at low shear rates.

Hans Joakim Skadsdem, Amare Leulseged, and Eric Cayeux (2019) measured and modelled the thixotropic behaviour of one OBM and WBM. For simplicity reasons, weighing material was not a constituent of the muds. The stress overshoot values were measured and plotted for a resting time of up to 30 minutes using Anton Paar MCR301 Rheometer with a smooth coaxial cylinder couetter geometry with rotating inner bob of outer diameter 26.653 mm and an open cup with smooth inner wall diameter of 28.919 mm. The rheometer was operated in controlled shear rate mode at constant fluid temperature of 293.15K [26].

Chapter 3: Methodology

The gel strength is measured as maximum stress overshoot by using the rheometer Anton Par MCR302. The details of the drilling muds, the process of taking, storing, and utilizing samples, the selection of various parameters, and specific details of the rheometer and geometry are used given in the following sections.

3.1 Drilling Muds Used in Experiments

In order to broaden the scope of this thesis work, three different muds were used for analysis. The muds are categorized under the rubric of Water Based Mud 1(WBM 1), Water Based mud (WBM 2) and Oil Based Mud (OBM). The further details of these muds can be found in sections 3.1.1, 3.1.2, and 3.1.3 respectively.

3.1.1 Water-Based Mud 1 (WBM 1)

This KCL Polymer Water Based Mud (WBM 1) contained crystalline Silica, quartz by 0.1-1% w/w in the solution. The mixture contained no other substance considered to be very persistent, bioaccumulating or toxic (PBT). The following are the properties of mud obtained from the safety data sheet of WBM 1.

Physical Properties

- Physical State = Liquid
- Color = Off white
- Odor = Odorless
- Specific gravity = 3.2

3.1.1.1 Sampling of WBM 1

The KCL polymer water-based mud (WBM 1) was taken to the Fluids Lab at the University of Stavanger (UiS). The mud was in a bottle of 05 liters as shown in figure 3.1.

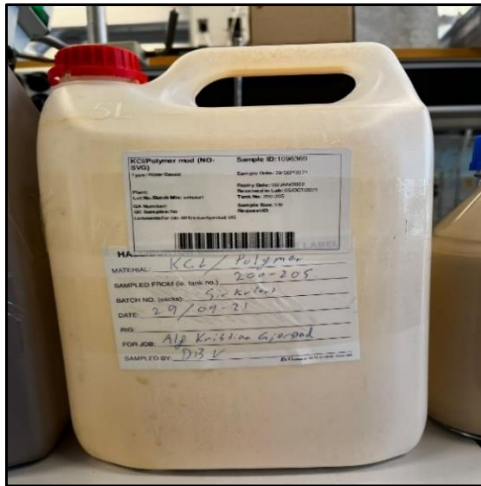


Figure 3.1 A 5-liter container of KCl Polymer WBM 1

The following steps were performed to take a representative sample out of the mud in a container.

- Shaked the container well
- Poured half of the mud from the container into a thoroughly cleaned bucket
- The rest of the mud in the container was shaken again to accommodate all the particles which may have settled down
- Poured all the mud from the container into the bucket
- Stirred the mud with a mixer for a period of 5-8 minutes
- From the bucket, divided the fluid into 6 separate bottles of 85 –900 mL each to take out a sample again easily as shown in figure 3.2.

Later on, experiments were performed to confirm the homogeneity of the sample. The details of which can be found in the section 4.1.



Figure 3.2 After mixing KCl Polymer WBM 1 and dividing into 6 bottles for storage

3.1.2 Water-Based Mud 2 (WBM 2)

The contents of KCL Polymer water-based mud (WBM 2) mud have been listed in table 3.1. It does not have any barite, a weighing material used in order to achieve desired mud properties. It means this mud can effectively be used for tests of longer resting times where the risk of particle sedimentation in the measurement geometry cannot be reduced. The following are the physical and chemical properties of mud.

Physical Properties

- Physical State = Liquid
- Color = Yellowish
- Odor = Odorless
- Specific gravity = 1.15

Chemical Properties

The mixture contains the following chemical substances, listed in the following table 3.1.

S. No.	Substance	Units	Contents (gram)
1	KCl Brine (1.15 SG)	g/l	690
2	Mil-Pac LV T	g/l	12
3	Xanthan Gum	g/l	3.5
4	Soda Ash	g/l	0.4
5	Lime	g/l	0.2
6	Chek-Trol	g/l	28
7	Water	g/l	360

Table 3.1 Contents of KCl Polymer WBM 2

Some key components have the tendency to affect the rheological properties of the fluid. For example, Xanthan Gum is characterized as a thickening agent in drilling muds to increase the viscosity of mud. It swells when reacts with water, acting as a gel-like structure which has an excellent tendency to carry the drill cuttings. It is important during static times, as it creates better gel strength to avoid the risk of cuttings to fall down due to gravity [3]. Furthermore,

Mil-Pac is commonly used in KCL Polymer WBM as fluid loss control agent. It serves the purpose of filtration control and is stable at temperatures to about 300°F [3].

3.1.2.1 Sampling of WBM 2

The original sample was present in a one liter container as shown in figure 3.3. It was taken into Rheology Lab for mixing at the UiS.

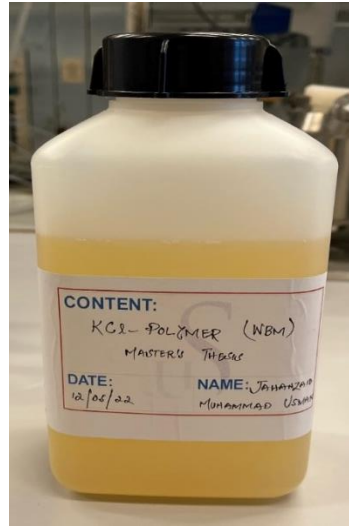


Figure 3.3 A 1-liter bottle of KCL Polymer WBM 2

According to safety rules and regulations as mentioned in the safety data sheet, we mixed the WBM 2 in the lab by using Heidolph Rotary equipment as shown in figure 3.4.

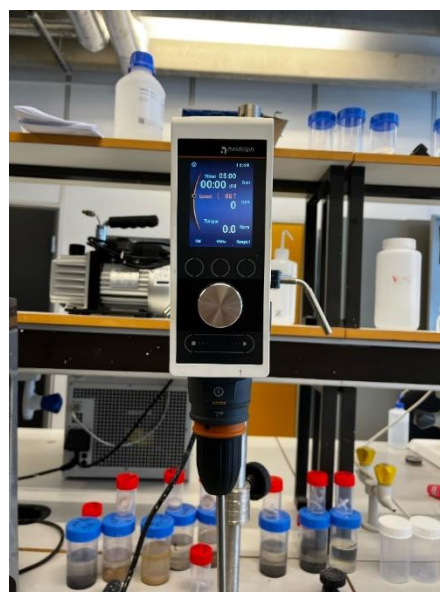


Figure 3.4 Heidolph Rotary equipment for mixing of KCL Polymer WBM 2

The mud was mixed by heidolph rotary equipment using the stirrer as shown in figure 3.5.



Figure 3.5 Type of stirrer to be used with Heidolph Rotary equipment

The following steps were performed to take a representative sample out of the mud in the container.

- Poured half of the mud from the one liter bottle into a thoroughly steel vessel
- Using Heidolph Mixture, rotating the stirrer with gradual speed of 200 rpm towards going to 1500 rpm in a span of 5 minutes. This ensured the homogenous mixing of the sample.
- The rest of the mud in the container was shaken again to accommodate all the particles which may have settled down
- Poured all the mud from the bottle into the vessel
- Stirred the mud with a Heidolph mixer for a period of another 5 minutes
- From the vessel, carefully put the mud back into one-liter bottle

3.1.3 Oil Based Mud (OBM)

The standard oil-based drilling fluid – ENVIROMUL Mud contains the following components listed in the table 3.2. This information is taken from the safety data sheet.

Sr. No	Substance	Contents (%)
1	Hydrocarbons, C14-C18, n-alkanes, iso alkanes, Cyclics aromatics	30-70
2	Calcium chloride	0-15
3	Fatty acid, tall-oil, Product with diethylenetriamine, maleic anhydrite	1-3
4	Distillates (petroleum) hydrotreated light	0-2
5	Calcium hydroxide	0-1
6	2-(2-Butoxyehoxy) ethanol	0-1
7	2-Butoxyehoxy ethanol	0-1

Table 3.2 Contents of Enviromul OBM

One of the key components in the table is Calcium chloride (CaCl_2) which is of paramount importance when it comes to lubricate and cool the bit during drilling. Additionally, it is extremely efficient in removing the cuttings from the well. It is also used to keep the formation pressure under control as it provides density in the mud.

3.1.3.1 Sampling of OBM

ENVIROMUL Oil-based mud (OBM) in 5-liter container as shown in figure 3.6 was taken to Rheology Lab.



Figure 3.6 A 5-liter container of Enviromul OBM

Following the safety protocols of handling the OBM, we performed the mixing as described below

- The 5 Liter mud container was shaken well and poured into a clean white bucket
- The mixer was run on 1500 RPM subsequently to allow the swift and homogenous mixing
- After 38 minutes of mixing, the mixture was poured into 6 flasks each of 850-900 mL
- Flasks were labeled and put into the refrigerator as shown in the figure 3.7.



Figure 3.7 After mixing Enviromul OBM and divided into 6 bottles for storage

3.2 Field Procedure of Gel Strength Measurement

In field, a viscometer is used to measure the gel strength of drilling fluids. Firstly, the drilling fluid is destructred at a high shear rate. Secondly, the fluid is set at rest typically for 10 seconds and 10 minutes. Thirdly, a rapid shear rate stepping from $0s^{-1}$ to $5s^{-1}$. Finally, the gel strength is recorded as the maximum shear stress during the start-up of flow [26].

In the lab, there are various ways of measuring gel strength. However, we used a procedure similar to the one used in the field work. The step-by-step details of the procedure are discussed in the section 3.4. In this thesis work, gel strength is reported as maximum stress overshoot.

3.3 Experimental Setup

The experiments were carried out by using Anton Paar MCR 302 and the data was plotted by Anton Paar RheoCompass software. The specification of some relevant components is provided in the following subsections.

3.3.1 Specification of the Rheometer

The Anton Paar MCR 302 is shown in figure 3.8. The Modular Compact Rheometer (MCR) is designed for a wide range of measurement tasks.



Figure 3.8 Anton Paar Modular Compact Rheometer (MCR) 302

It comes with software Anton Paar RheoCompass (RHEOPLUS/32 V3.62) which automatically recognizes and configures the system. To maintain temperature, the rheometer is also equipped with an air supply as shown in figure 3.9.



Figure 3.9 Setup showing the air supply equipment to Anton Paar MCR 302

To perform tests, the rheometer with a smooth cocentric cylindrical measuring system (discussed in section 3.3.2.1) was used.

The following are some of the other specific details of the component used in this thesis.

- Diameter of measuring bob = 26.653 mm
- Length of measuring bob = 40.032 mm
- Diameter of the cup = 28.910 mm

The rheometer was operated in controlled shear rate mode at constant fluid temperature of 20 degree centigrade (293.15K).

3.3.2 Sample Loading Systems

There are four sample loading systems available in the rheometer.

3.3.2.1 Cocentric Cylinder System

The sample is loaded in the cup up to the mark provided therein. The measuring bob is lowered and immersed in the sample. This system looks like as shown in figure 3.10.

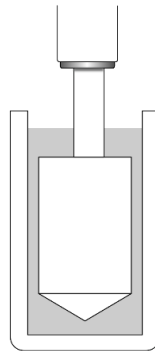


Figure 3.10 Illustration of cocentric cylinder system

Advantages	Disadvantages
No sample drying effects	High sample volume required
Uniform temperature within entire cup	Entrapement of air bubbles
No gap leakage at high shear rates	Turbulences at high shear rates

Table 3.3 Pros and cons of cocentric cylinder system

In this thesis, concentric cylinder system is used for all experiments.

3.3.2.2 Plate-Plate System

A plate system is shown in figure 3.11. The sample is placed just outside the rim of the measuring system. All excess sample is removed; the measuring system is moved to the measuring position.

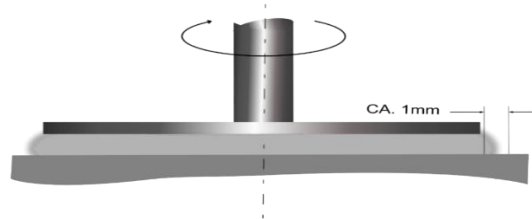


Figure 3.11 Illustration of Plate-Plate system

Advantages	Disadvantages
Suitable for highly viscous samples	Gap leakage at higher shear rates
Small sample volume	Variable shear rates within the gap
Quick temperature equilibration	Sample drying effect

Table 3.4 Pros and cons of plate-plate system

3.3.2.3 Cone-Plate System

A cone system is shown in the figure 3.12. The sample is placed just outside the rim of the measuring system. All excess sample is removed; the measuring system is moved to the measuring position. Both too much and too little samples could lead to large errors in the measurement data.

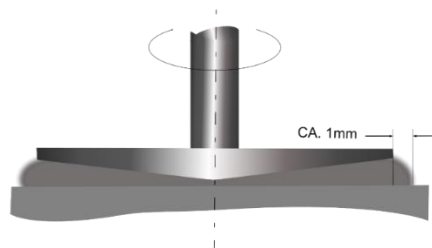


Figure 3.12 Illustration of Cone-Plate System

Advantages	Disadvantages
Constant shear rate	Gap leakage at higher shear rates
Small sample volume	Variable shear rates within the gap
Quick temperature equilibration	Sample drying effect

Table 3.5 Pros and cons of cone-plate system

3.3.2.4 Double Gap System

A double gap system is shown in the figure 3.13. A small amount of sample is put in the gap of the cup. And then the measuring bob is lowered in the cup; excess sample is removed.

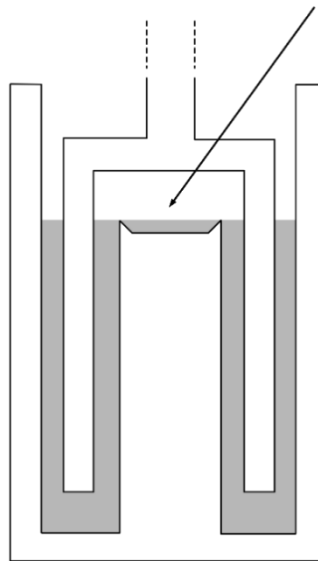


Figure 3.13 Illustration of Double Gap system


Advantages	Disadvantages
Suitable for low viscous samples	Sample drying effect
Accurate temperature within the entire cup	Slow temperature equilibration
Small gap	Turbulent at high shear rates

Table 3.6 Pros and cons of double-gap system

3.4 Experimental Procedure

The following is the step by step by procedure before selecting the parameters to run a specific test.

3.4.1 Preliminary Steps

- Keep the mud sample bottle at room temperature
- Turn on the air supply and the rheometer
- Launch the Rheoplus software
- Load the sample into the rheometer
- Plug in the measuring system
- From the control panel as shown in figure 3.14 of the Rheoplus software perform the following steps
 - Initialize the rheometer by pressing the **Initialize** button
 - Reset temperature to 20° C and normal force to 0.00 N
 - Press the downward arrow button to lower the measuring system into the sample by pressing 
- Set the experimental parameters to perform the test

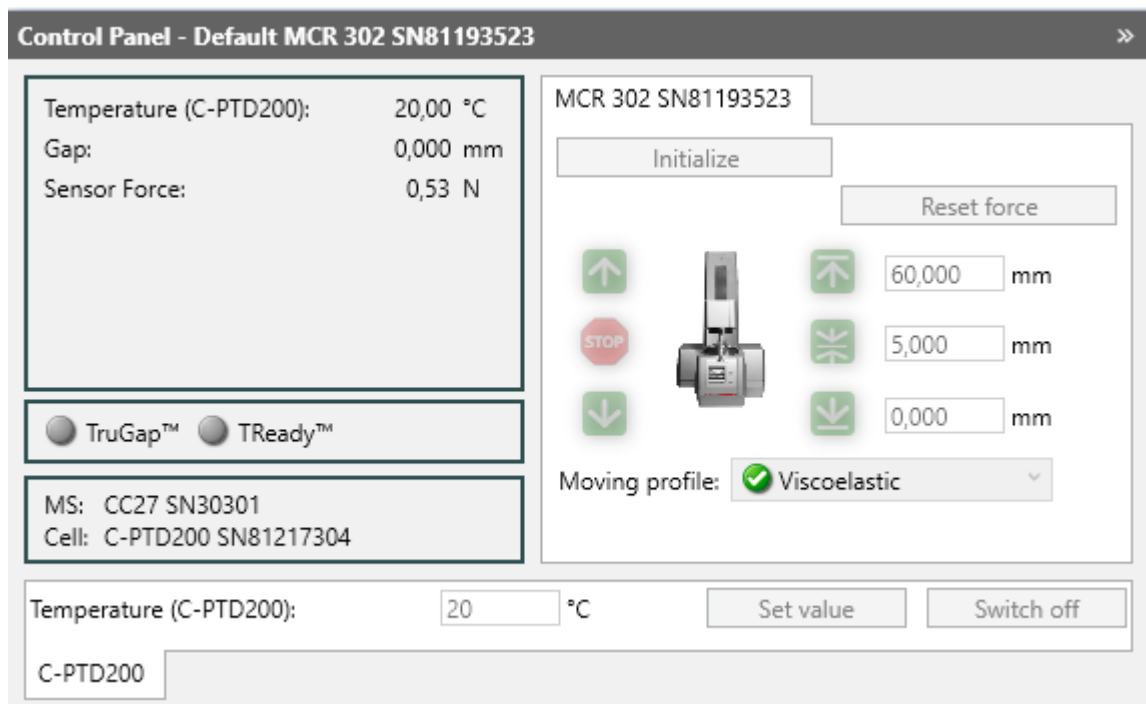


Figure 3.14 Control Panel of MCR 302 Software

3.4.2 Measuring Steps

After preliminary steps, all experiments have four steps in which certain parameters were selected. The details and findings of how the impact of the various parameter was observed and will be discussed in the next chapter. However, the summary of the steps is as below

1. Select the timing of the initial shear rate. The purpose of this step is to overcome any predeveloped microstructures in the sample which may have developed due to resting.
2. Select the resting time so that gelling properties could be developed in the sample fluid.
3. Select the linear shear rate. After the second step, gelling starts in the mud. In this step, by providing linear shear rate, stress overshoot is estimated. At the highest point, the disturbing forces overcome the viscous forces amongst the molecules and fluid starts flowing again.
4. Apply constant shear rate. In this step, a constant shear rate is applied so that gradually both forces become equal.

Chapter 4: Selection of Parameters

The main objective of our work is to analyze gelling properties of drilling. In this regard, one of the key parameters under consideration is resting time. However, a step-by-step, methodical and analytical approach was used to determine the impact of various other parameters on gel strength. To achieve consistent results, the homogeneity of the samples taken from various flasks was tested and confirmed. The experiments mentioned in this chapter were performed on KCL Polymer Water-Based mud (WBM 1). The steps of the testing and other relevant details are discussed in the following subsections.

4.1 Homogeneity Conformity

The purpose of these tests is to ensure that a sample taken out of any flasks is a representative sample. During the sampling process, we arranged samples in six different bottles namely bottle 1, bottle 2 til bottle 6.

For this task, we took samples from three different bottles namely bottle numbers 2, 4, and 6 and kept all other parameters constant while running the tests. The following are the parameters of the tests recorded in table 4.1, and the results are shown in figure 4.1.

Test No.	Sample Bottle no.	Initial Shear Rate Time (min)	Resting Time (seconds)	Linear Acceleration of Shear Rate	Constant Shear Rate (per second)	Max. Stress Overshoot (Pa)
1	2	5	60	0 to 2 in 0.5 seconds	2	1.464
2	6	5	60	0 to 2 in 0.5 seconds	2	1.46
3	4	5	60	0 to 2 in 0.5 seconds	2	1.464

Table 4.1 Homogeneity conformity testing summary

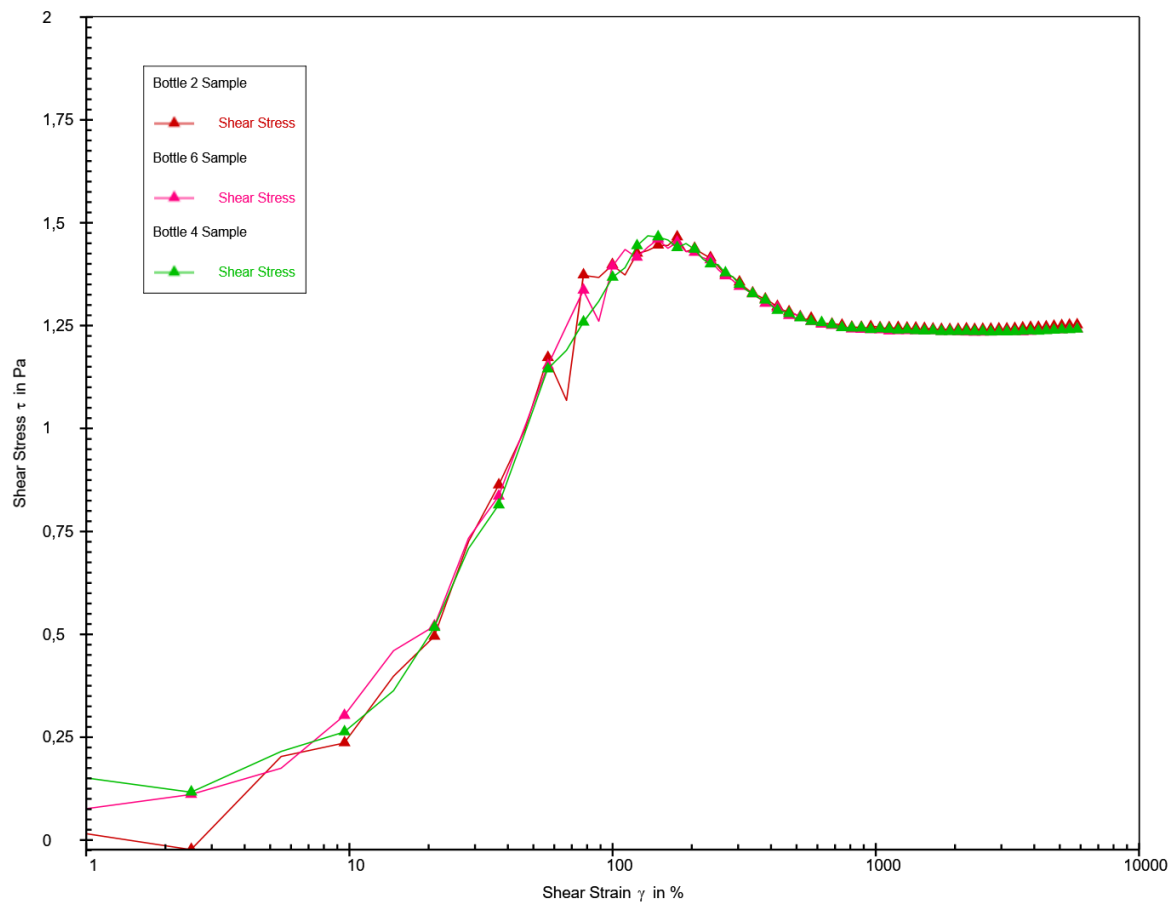


Figure 4.1 Stress overshoots resembling homogeneous response from different samples

As seen in figure 4.1 the difference between gel strengths are negligible. Hence, the homogeneity is confirmed.

4.2 Initial Shear Rate Time Testing

In all the experiments performed in this thesis, the first step is to apply the initial shear rate to overcome any microstructure which may have been developed in the mud due to resting. Since fluid history affects its thixotropic properties, this parameter was tested in detail. Initially, four different tests were performed. In these tests, we increased the resting time gradually from 2 minutes to 10 minutes. The following are the parameters of the tests, and the results are shown in table 4.2 and figure 4.2.

Test No.	Initial Shear Rate Time (min)	Resting Time (seconds)	Linear Acceleration of Shear Rate	Constant Shear Rate (per second)	Max. Stress Overshoot (Pa)
3	2	60	0 to 2 in 0.5 seconds	2	1.496
4	3	60	0 to 2 in 0.5 seconds	2	1.472
5	5	60	0 to 2 in 0.5 seconds	2	1.452
6	10	60	0 to 2 in 0.5 seconds	2	1.396

Table 4.2 Initial Shear Rate testing summary in ascending order

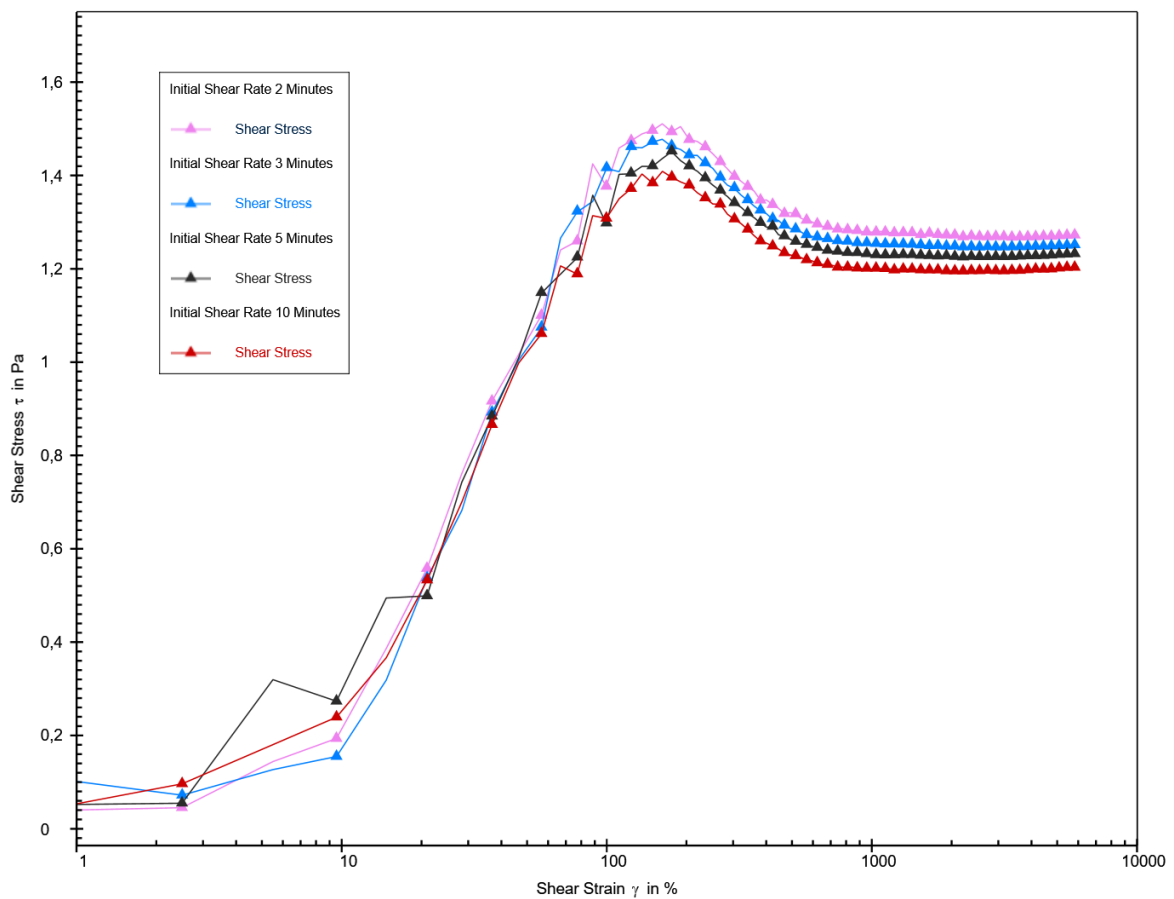


Figure 4.2 Stress overshoots following different initial shear rates (increasing order)

As seen in figure 4.2, with increasing time of the shear rate, the value of stress overshoot decreased. This is apparently due to the fact that thixotropic behaviour is time and history-dependent.

In the next step of this phase, we came up with four more tests. In these tests, instead of increasing the initial shear rate time gradually, we decreased the initial shear rate time gradually from 10 minutes to 02 minutes to confirm the repeatability of the results. The following are the parameters of the tests, and the results are shown in table 4.3 and figure 4.3.

Test No.	Initial Shear Rate Time (min)	Resting Time (seconds)	Linear Acceleration of Shear Rate	Constant Shear Rate (per second)	Max. Stress Overshoot (Pa)
7	10	60	0 to 2 in 0.5 seconds	2	1.424
8	5	60	0 to 2 in 0.5 seconds	2	1.439
9	3	60	0 to 2 in 0.5 seconds	2	1.454
10	2	60	2	1.477	

Table 4.3 Initial Shear Rate testing summary in descending order

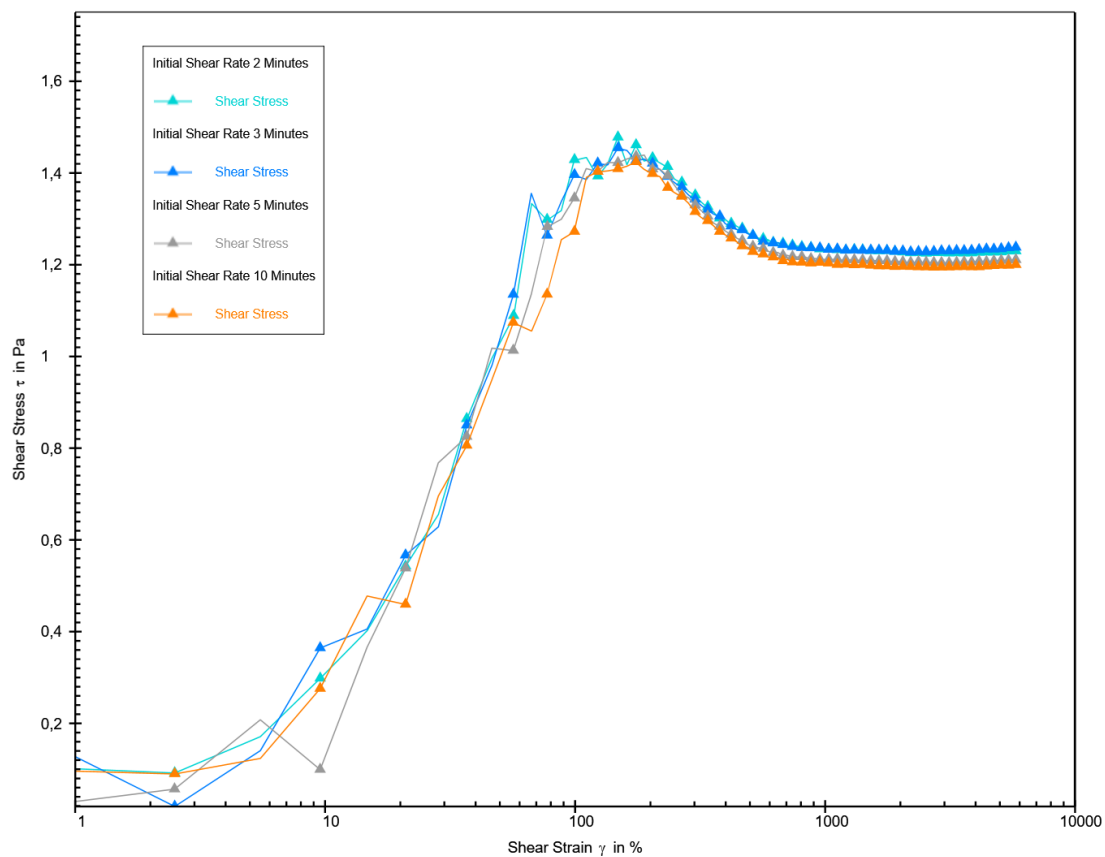


Figure 4.3 Stress overshoots following different initial shear rates (decreasing order)

This time by decreasing the initial shear rate gradually, the value of maximum stress overshoot increased.

Summary

The initial shear rate affects the maximum value of stress overshoot. Initially, it was observed that by increasing the time of the initial shear rate, the value of stress overshoot decreased. Upon executing the tests in the consecutive decreasing way, the value of maximum stress overshoot increased.

With more initial shear rate time, there will be more uniformity in the fluid and hence less micro structure in the fluid. This will lead to a more accurate estimation of gel strength as compared to when tested at low initial shear rate times. For this reason, for all final tests in Chapter 5, we used an initial shear rate of five minutes.

The value of stress overshoot and the difference between the values at the same time is reported in the following table below and figure 4.4.

Increasing time		Decreasing time		Difference (Pa)
Initial Shear Rate Time (min)	Stress Overshoot Value (Pa)	Initial Shear Rate Time (min)	Stress Overshoot Value (Pa)	
2	1.496	2	1.424	0.072
3	1.472	3	1.439	0.033
5	1.452	5	1.454	-0.002
10	1.396	10	1.477	-0.081

Table 4.4 Comparison of initial shear rate variation with respect to time

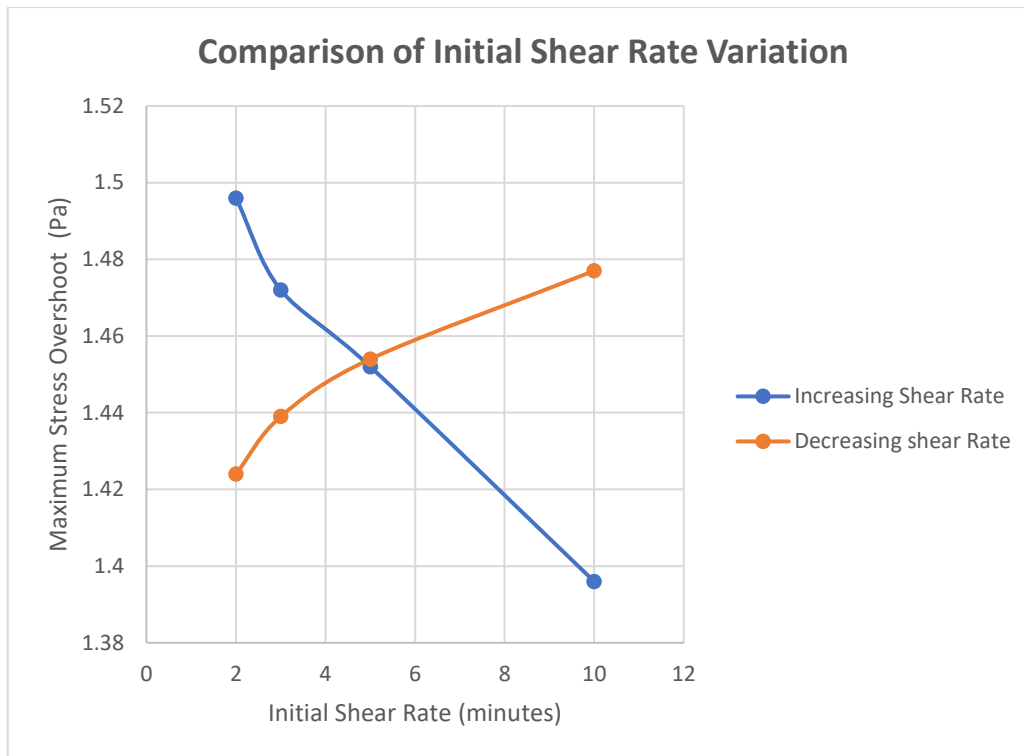


Figure 4.4 Comparison of initial shear rate variation with respect to time

4.3 Local Temperature Effects

Before running the test, the temperature is set and controlled at 20 degrees centigrade on the Rheometer. However, during the tests, there may exist a local difference in the mud sample placed inside a cup in the Rheometer. Therefore, local temperature could affect the value of maximum stress overshoot.

Furthermore, in the previous section of initial shear rates testing, it was observed that with increasing initial shear rate gradually, the maximum value of stress overshoot kept on decreasing. On the other hand, it was also observed that by decreasing the initial shear rate gradually, the maximum value of stress overshoot increased. Since the tests were run consecutively, there was a probability that the local temperature effect on mud particles might be contributing to the value of maximum stress overshoot.

To understand the impact of local temperature effect on the results, two more tests were executed. Then, we compared the results with the tests which were performed in the previous section 4.2.

Firstly, after the gap of 8 hours, we ran a test in which the initial shear rate time was 2 minutes. The following are the parameters of the test.

Test No.	Initial Shear Rate Time (min)	Resting Time (seconds)	Linear Acceleration of Shear Rate	Constant Shear Rate (per second)	Max. Stress Overshoot (Pa)
11	2	60	0 to 2 in 0.5 seconds	2	1.494

Table 4.5 Local Temperature Effect testing Summary with 2 minutes applied initial shear rate

Now, we want to compare the result of this test (Test no. 11) with Test no. 3 and Test no. 10 which are taken from section 4.2 as those tests were run by using the same parameters. A summary of the comparison in tabular and graphical format is presented in table 4.6 and figure 4.5.

Test No.	Initial Shear Rate Time (min)	Resting Time (seconds)	Linear Acceleration of Shear Rate	Constant Shear Rate (per second)	Max. Stress Overshoot (Pa)
3	2	60	0 to 2 in 0.5 seconds	2	1.496
10	2	60	0 to 2 in 0.5 seconds	2	1.477
11	2	60	0 to 2 in 0.5 seconds	2	1.494

Table 4.6 Comparison of Stress overshoots of 2 minutes applied initial shear rate indicating local temperature effect

Test no. 3 was the first test in increasing order. This means that this test was run on a fresh sample. And also, test no. 11 was run on a fresh sample with the same parameters. Hence, the results of these two tests are quite similar as shown in table 4.6 and figure 4.5.

On the other hand, test no.10 was the last test in decreasing order. This means that four more tests were already run on the fluid sample which may have increased the local temperature of the certain particle of the sample. Therefore, for test nos. 10 and 11, although the parameters are the same, the maximum value of stress overshoot is not as close as observed in the case of

tests nos. 3 and 11. This implies that certain local temperature differences in temperature may exist in the fluid sample.

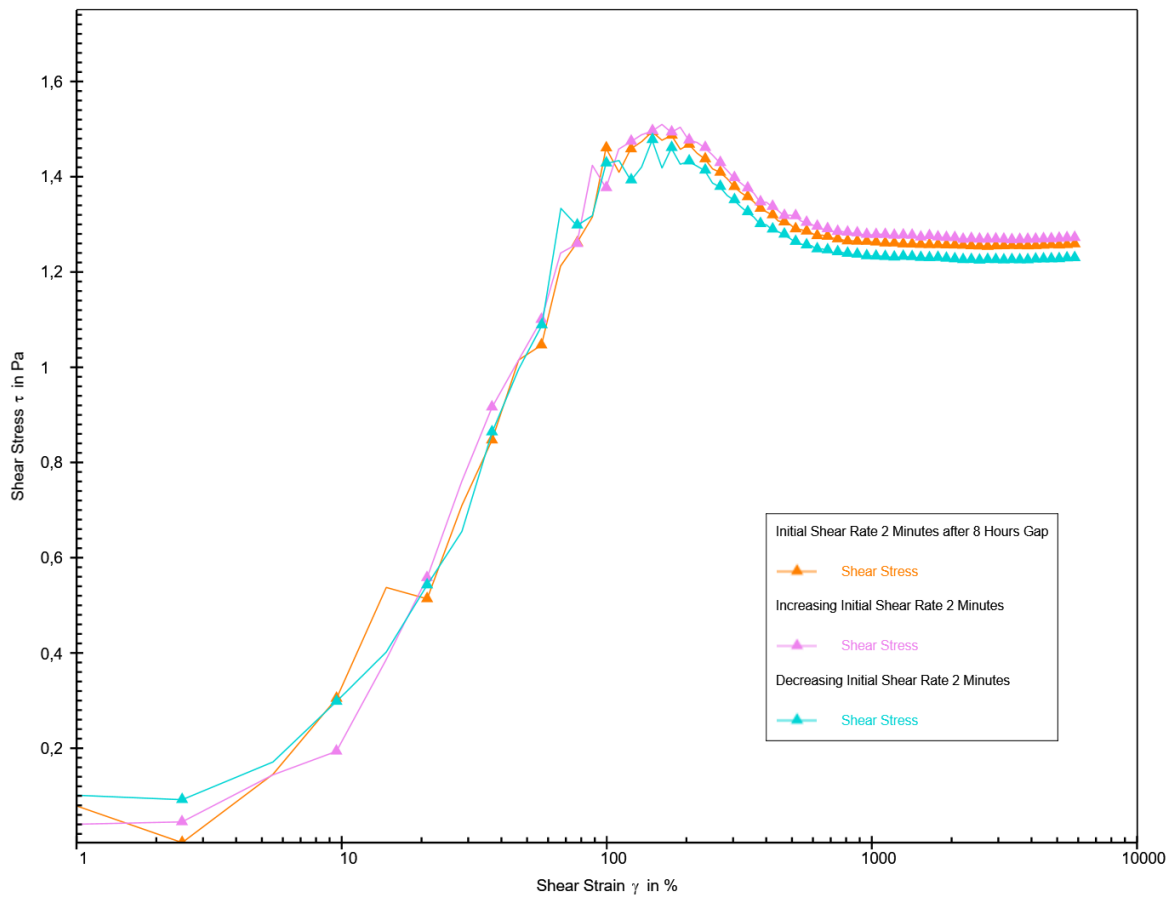


Figure 4.5 Comparison of Stress overshoots of 2 minutes applied initial shear rate indicating local temperature effect

Secondly, to further clarify the impact of local temperature effects, after the gap of 8 hours, we ran another test in which the initial shear rate was applied for 5 minutes. The following are the parameters of the test.

Test No.	Initial Shear Rate Time (min)	Resting Time (seconds)	Linear Acceleration of Shear Rate	Constant Shear Rate (per second)	Max. Stress Overshoot (Pa)
12	5	60	0 to 2 in 0.5 seconds	2	1.46

Table 4.7 Local Temperature Effect testing Summary with 5 minutes applied initial shear rate

Now, we want to compare the result of this test (Test no. 12) with Test no. 5 and Test no. 8 which are taken from section 4.2 as those tests were run by using the same parameters. A summary of the comparison in tabular and graphical format is presented in table 4.8 and figure 4.6.

Test No.	Initial Shear Rate Time (min)	Resting Time (seconds)	Linear Acceleration of Shear Rate	Constant Shear Rate (per second)	Max. Stress Overshoot (Pa)
5	5	60	0 to 2 in 0.5 seconds	2	1.452
8	5	60	0 to 2 in 0.5 seconds	2	1.439
12	5	60	0 to 2 in 0.5 seconds	2	1.46

Table 4.8 Comparison of Stress overshoots of 5 minutes applied initial shear rate indicating local temperature effect

Test no. 12 was run on a fresh sample for 5 minutes.

Test no. 5 was the third test in increasing order. This means that two tests of initial shear rate 2 minutes and 3 minutes (total initial shear rate time = 5 minutes) were already run on the sample.

Test no. 8 was the second test in decreasing order. One test of initial shear rate time of 10 minutes was already executed on the sample.

One could argue that the result of test no. 12 would be closer to test no. 5 because there is a possibility of a less local temperature effect as compared to test 8. Table 4.8 and figure 4.6 illustrate the same findings.

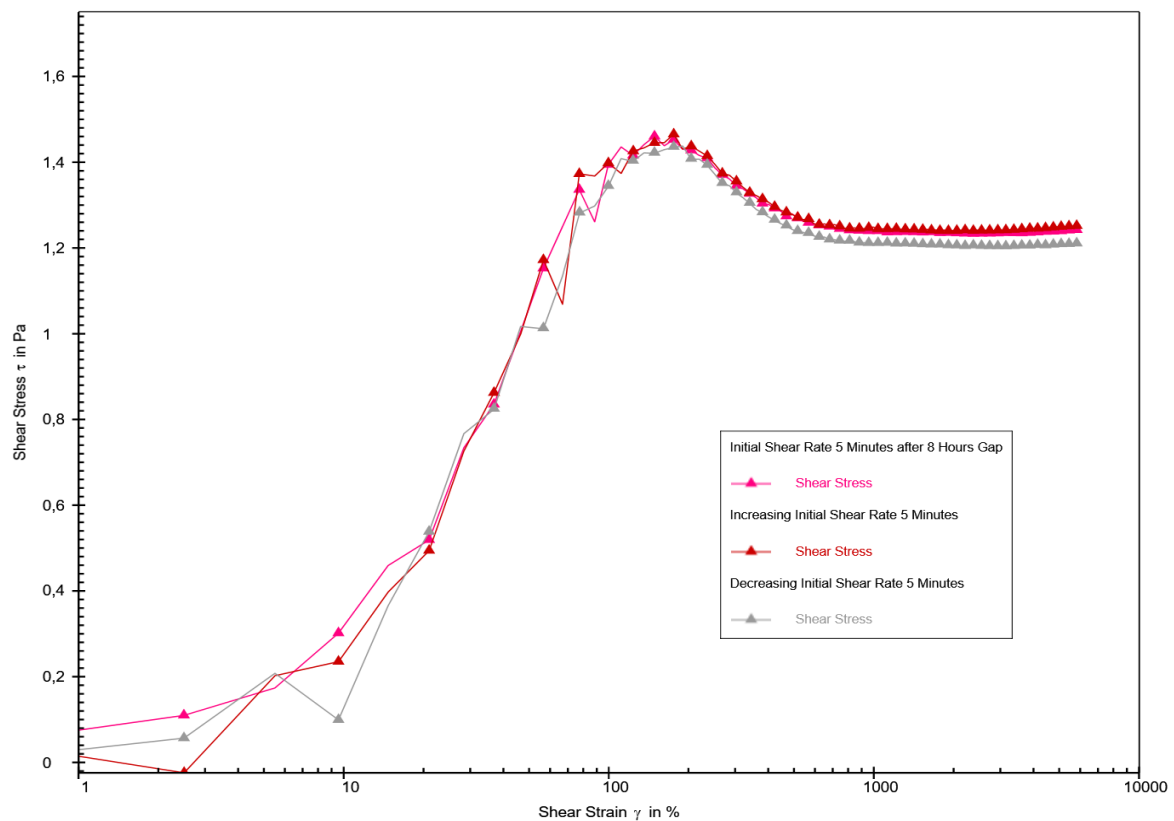


Figure 4.6 Comparison of Stress overshoots of 5 minutes applied initial shear rate indicating local temperature effect

Summary

Although Rheometer controls the temperature, due to changing initial shear rate time, there is a certain effect of local temperature on the fluid sample. This may lead to the difference in the value of gel strength measured in terms of maximum stress overshoot. To have minimal impact of local temperature effect on results, we took fresh samples from a bottle which was kept at room temperature for at least 10 minutes.

4.4 Linear Acceleration Testing

In the third step of the testing methodology, linear acceleration is provided to start-up the flow. In the literature, Skasdem (2019) performed experiments by increasing linear acceleration from 0 to $2s^{-1}$ in 0.5 seconds, and then maintained it for $2s^{-1}$ for additional 30 seconds.

We performed a series of experiments to understand how changing the value and time of shear rate can impact the gel strength.

4.4.1 Maximum Stress Overshoot vs. Resting Time

In this stage, we measured the maximum value of stress overshoot by increasing the resting times for three different values of shear rate.

4.4.1.1 Shear Rate Increment from 0 to 0.5 per second in 0.5 seconds

The following parameters were used for the testing purpose, and the results are shown in table 4.9 and figure 4.7.

Test No.	Initial Shear Rate Time (min)	Resting Time (minutes)	Linear Acceleration of Shear Rate	Constant Shear Rate (per second)	Max. Stress Overshoot (Pa)
16	3	2	0 to 0.5 in 0.5 seconds	0.5	0.827
17	3	5	0 to 0.5 in 0.5 seconds	0.5	0.903
18	3	10	0 to 0.5 in 0.5 seconds	0.5	0.95

Table 4.9 Shear rate increment from 0 to 0.5 per second testing summary

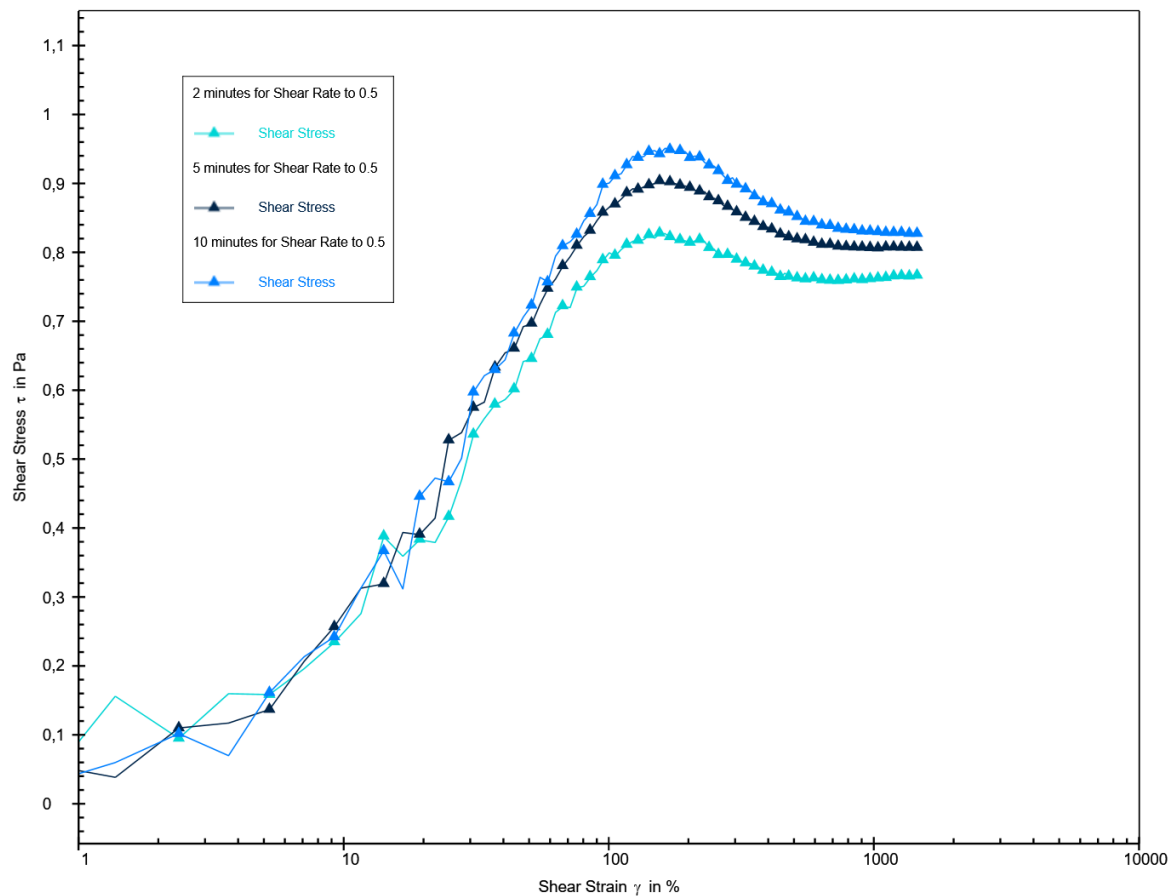


Figure 4.7 Stress overshoots following shear rate increment from 0 to 0.5 per second

As seen from figure 4.7, at a constant shear rate, by varying the resting time, the values of maximum stress overshoot increase. However, it can be observed that the overall range of the values is significantly low that is from 0.827 Pa to 0.95 Pa.

4.4.1.2 Shear Rate Increment from 0 to 2 per second in 0.5 seconds

The following parameters were used for the testing purpose in table 4.10, and the results are shown in figure 4.8.

Test No.	Initial Shear Rate Time (min)	Resting Time (minutes)	Linear Acceleration of Shear Rate	Constant Shear Rate (per second)	Max. Stress Overshoot (Pa)
19	3	2	0 to 2 in 0.5 seconds	2	1.548
20	3	5	0 to 2 in 0.5 seconds	2	1.651
21	3	0 to 2 in 0.5 seconds	2	1.749	

Table 4.10 Shear rate increment from 0 to 2 per second testing summary

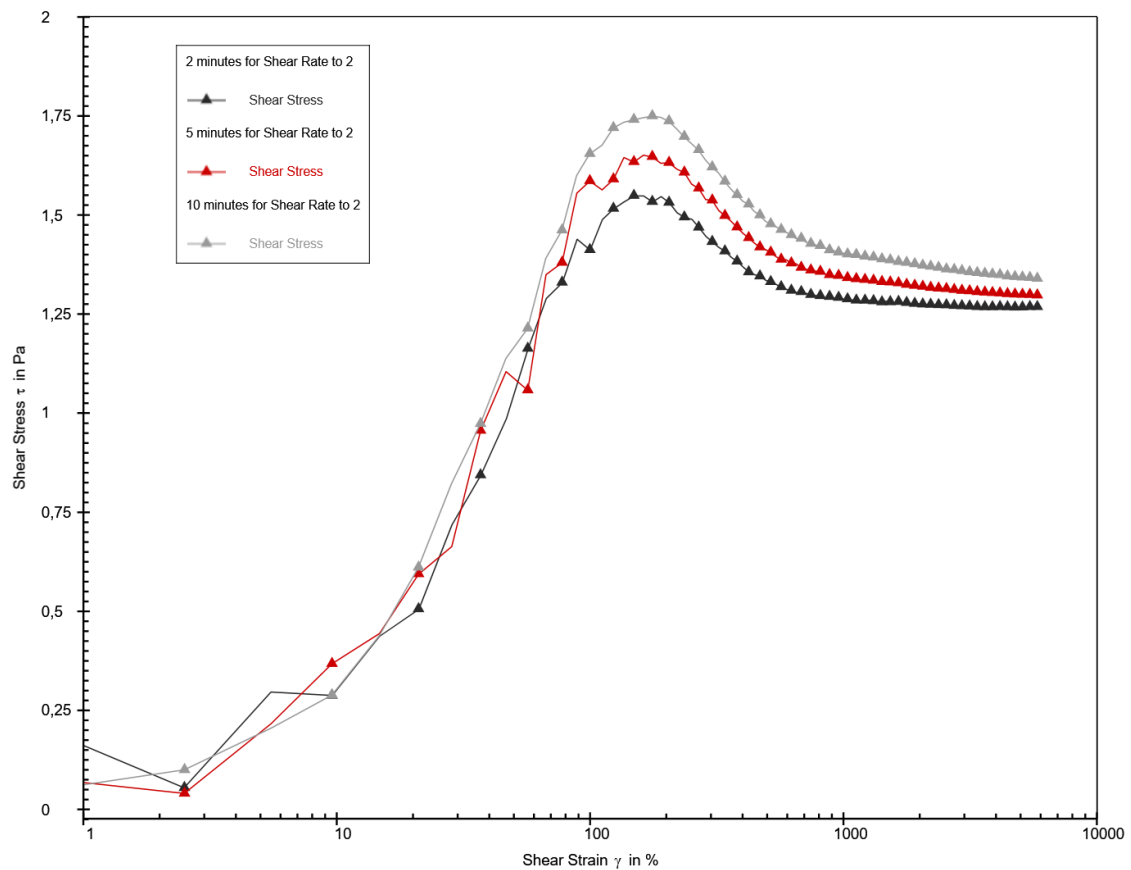


Figure 4.8 Stress overshoots following shear rate increment from 0 to 2 per second

It is evident from the table and figure that at a constant shear rate, by varying the resting time, the values of maximum stress overshoot increase. It can be observed that the overall range of the values is significantly low that is from 1.548 Pa to 1.749 Pa. The values and trend indicate that changing the acceleration has some effect on the values of maximum stress overshoot which can be further analyzed.

4.4.1.3 Shear Rate Increment from 0 to 5.1 in 0.5 seconds

As discussed in the field procedure (section 3.2), after the period of rest, the mud is subjected to a rapid shear rate step from 0s^{-1} to 5.1s^{-1} . We attempted to simulate the conditions in the lab as well. The overall approach was to increase the shear rate from 0s^{-1} to 5.1s^{-1} by changing the resting time for each of the tests. The following are the parameters of the tests in table 4.11 and the results are shown in figure 4.9.

Test No.	Initial Shear Rate Time (min)	Resting Time (minutes)	Linear Acceleration of Shear Rate	Constant Shear Rate (per second)	Max. Stress Overshoot (Pa)
22	3	2	0 to 5.1 in 0.5 seconds	5.1	2.443
23	3	5	0 to 5.1 in 0.5 seconds	5.1	2.521
24	3	10	0 to 5.1 in 0.5 seconds	5.1	2.608

Table 4.11 Shear rate increment from 0 to 5.1 per second testing summary

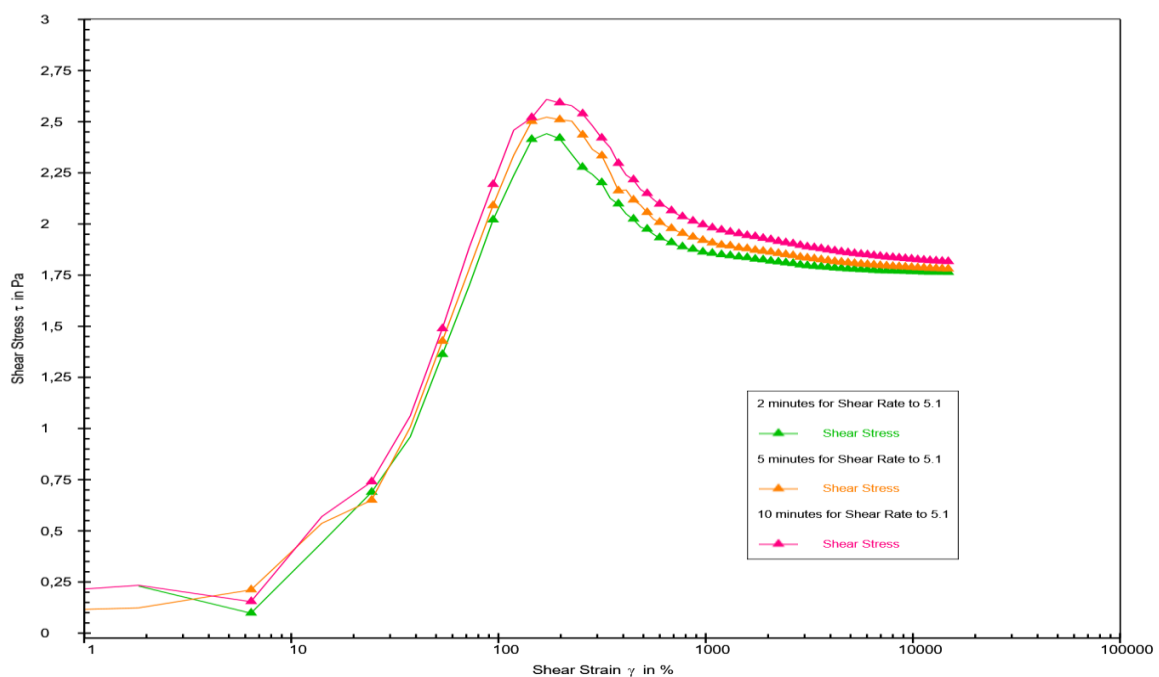


Figure 4.9 Stress overshoots following shear rate increment from 0 to 5.1 per second

As it is clear from figure 4.9, increasing the shear rate increased the value of maximum yield stress. At 2, 5, and 10 minutes, the gel strength values are 2.443 Pa, 2.521 Pa, and 2.608 Pa respectively. If we compare the results of test 21 (the value mostly used by some authors) and test 24 (the values corresponding with field operations), the gel strength increased by a factor of 0.859 Pa. This makes linear acceleration a point to be considered for future tests and modelling.

4.4.1.4 Summary

By increasing the resting and shear rate value, maximum value of stress overshoot increases as displayed in the figure 4.10.

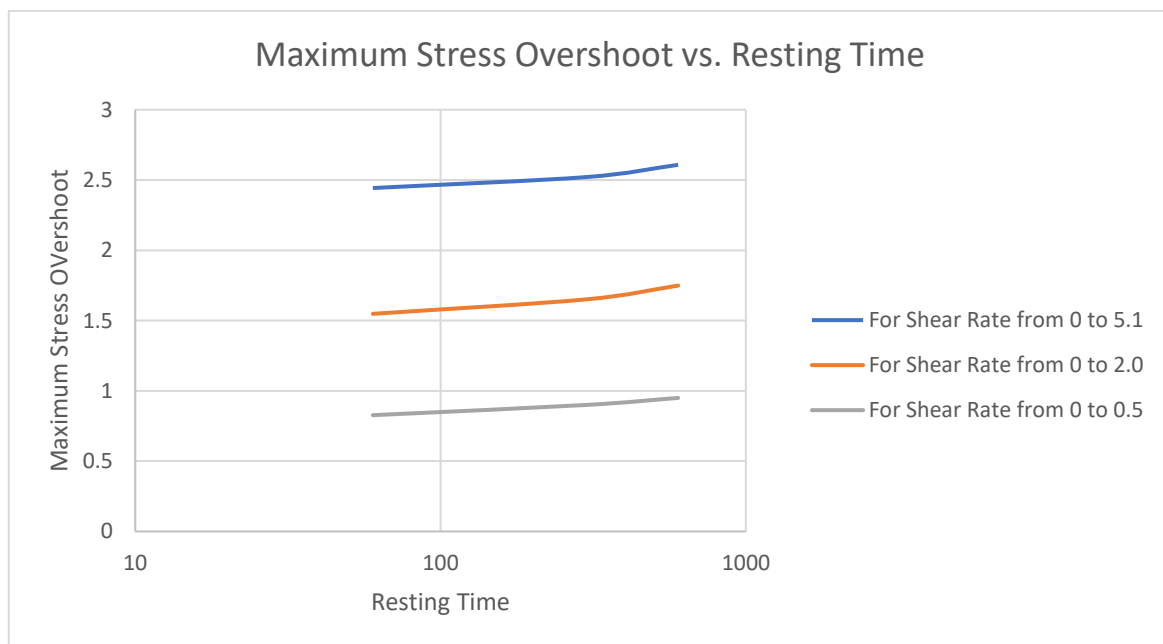


Figure 4.10 Comparison of stress overshoots following different shear rate increments

We can observe that by increasing the resting time stress overshoot values increased significantly. Having said this, linear increment of shear rate does affect the value of gel strength. Therefore, due consideration must be made while selecting the values for this parameter.

4.4.2 Testing at Extremely Low Shear Rate Value

In this last step of this process, we wanted to examine the impact of extremely low shear rate on gel strength. The following parameters were used to run the test.

Test No.	Initial Shear Rate Time (min)	Resting Time (min)	Linear Acceleration of Shear Rate	Constant Shear Rate (per second)	Max. Stress Overshoot (Pa)
25	3	10	0 to 0.001 in 0.5 seconds	0.001	N/A

Table 4.12 Extremely low shear rate testing summary

The curve could not be constructed to determine the maximum value of yield stress.

4.5 Conclusion

By and large, it is concluded that gel strength being a thixotropic property depends upon several factors. Fluid shear history is one of those factors. By changing the initial shear rate time, the values of maximum stress overshoot vary. Similarly, the linear acceleration of shear rate may impact gel strength value. Moreover, the local temperature effect on the mud sample could also contribute to the difference in maximum stress overshoot value. From the extensive testing performed in this work, it is suggested that this parameter should be selected with utmost care. For example, under the same conditions, the maximum value of stress overshoot was observed to be much greater while a higher shear rate was applied that is from 0 to 5.1s^{-1} . Lastly, the maximum value of stress overshoot is also influenced by the resting time.

Chapter 5: Experimental Results and Discussion

In this chapter, experimental results, and a discussion on three different muds used in this research work are provided. The testing procedure and other relevant details have been discussed in section 3.4. Followed by the presentation of the results, conclusion for each of the mud samples is provided. Finally, further work recommendations are presented at the end of the chapter.

5.1 WBM 1

WBM 1 is the same mud on which we performed all our experiments recorded in chapter 4. Here, we continued with the same mud and used the following parameters for testing.

- Initial shear rate = 5 minutes
- Resting time = Varied for every test. The maximum resting time is 14400 seconds (4 hrs)
- Linear shear rate = 0 to 2 per second in 0.5 seconds and maintained for additional 30 seconds

The results of maximum stress overshoot against varying times are shown in table 5.1 and figure 5.1.

WBM 1	
Time (sec)	Max Stress overshoot (Pa)
20	1.19
30	1.255
60	1.353
120	1.431
300	1.731
600	1.825
1200	2.043
1800	2.131
3600	2.402
7200	2.599
10800	2.757
14400	2.892
21600	3.13

Table 5.1 Stress overshoots in the WBM 1 following different resting times

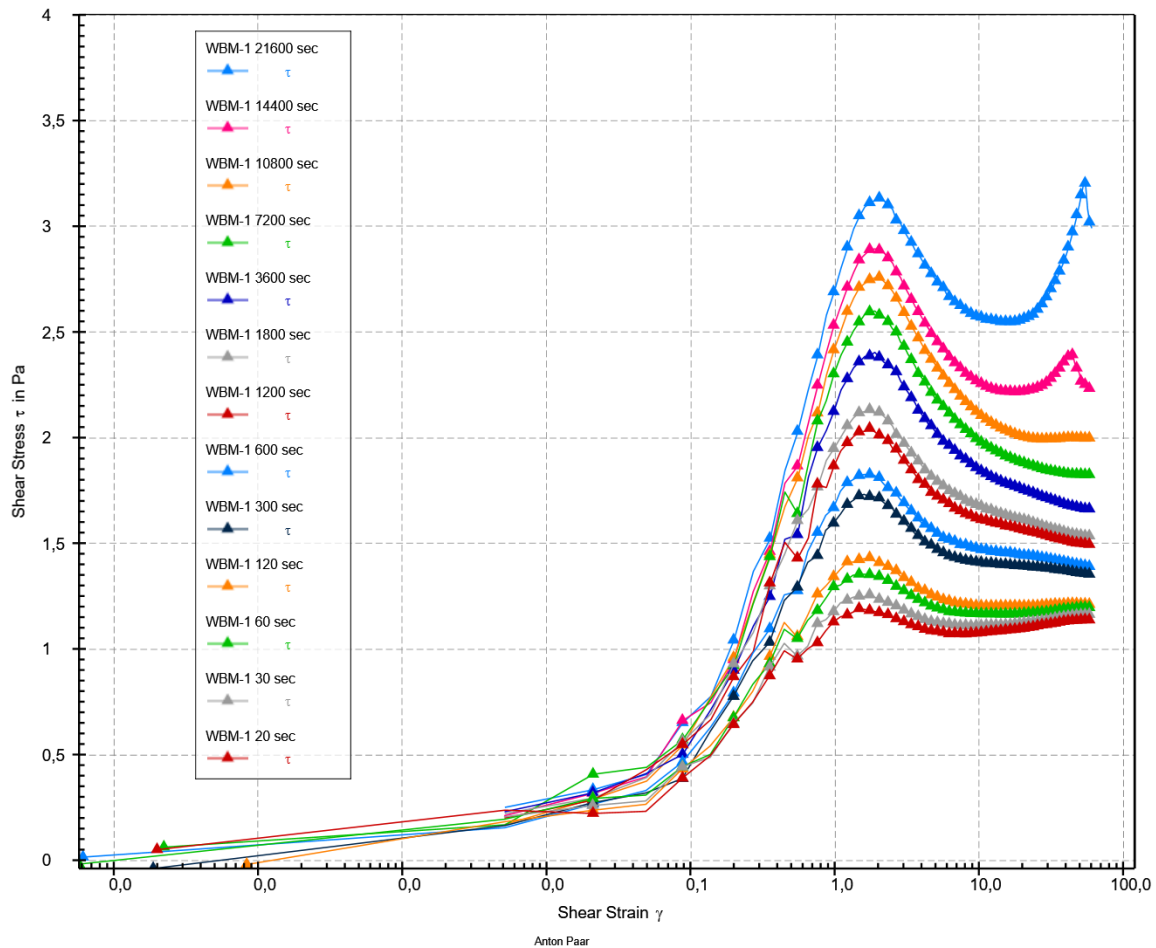


Figure 5.1 Stress overshoots in the WBM 1 following different resting times

Discussion

From the figure shown above, the following are some points for consideration.

Firstly, by increasing the resting time, the maximum value of stress overshoot keeps on increasing. As mostly observed in the literature, the maximum resting time is 30 minutes. In this case, the maximum values of stress overshoot at 30 minutes and 14400 seconds (4 hours) are 2.131 Pa and 3.130 Pa respectively. In short, the gel strength measured in terms of maximum stress overshoot increased by 1.0 Pa. This may have serious implications if the mud remained stationary for hours in the well. For example, excessive pump pressure than expected would be required to initiate the flow after the stationary period. This excessive pump rate may fracture the formation in open hole.

Secondly, towards the right end of the graph, the curves are not converging towards each other. Rather than converging, separation keeps on widening with the increased resting time.

We are not completely sure about this behaviour. However, we have one possible explanation. During the mixing, the polymer structure may have been broken down. Therefore, we suggest for any further research work, mixing should be done more carefully to avoid any micro-level damage to the structure of polymers.

Thirdly, for the curves pertaining to the resting time of 4 and 6 hours, there is another peak in the latter half of the curve as well. After the initial peak, the stress value decreases but starts to increase again until the second peak is achieved. After that, the stress value continues to decay. One proposition is that for longer hours, the heavy particles in the mud sample have settled down thereby changing the composition of mud significantly would lead to flow heterogeneities or shear bands. If the components of the mud were known, more investigation with respect to weighing and viscous material could have helped in further understanding.

Lastly, we can find that the maximum value of stress overshoot increased logarithmically with the increased resting time. However, at higher resting times such as 2 hours and later, the trend deviates farther from the logarithmic pattern and keeps on increasing. This is shown in figure 5.2

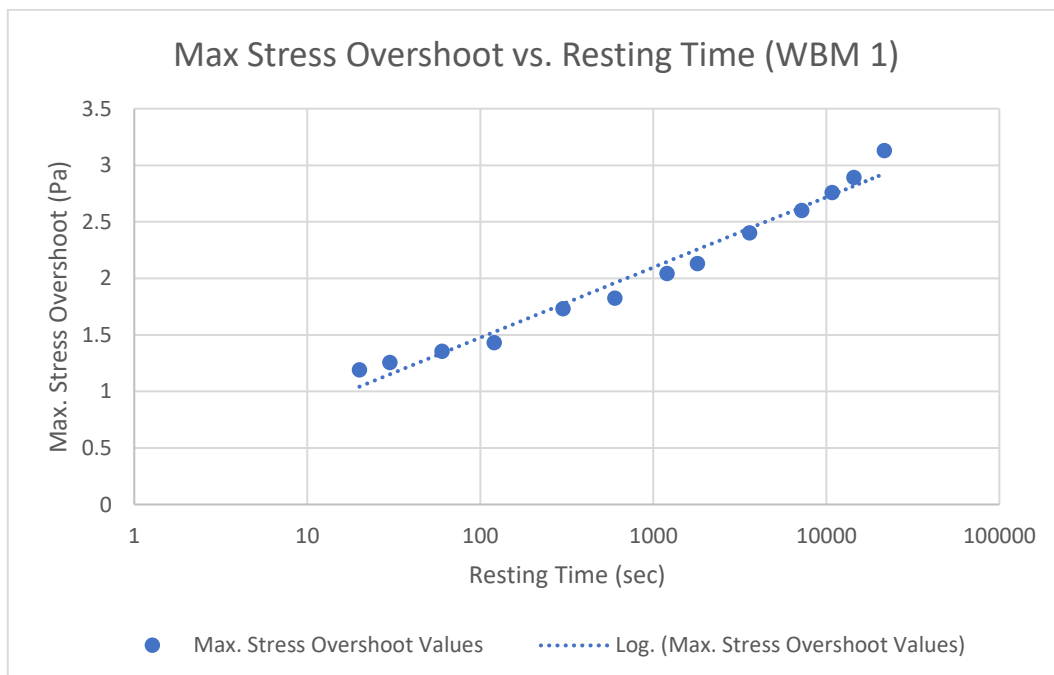


Figure 5.2 Maximum Stress overshoots in the WBM 1 as logarithmic function following different resting times

5.2 WBM 2

WBM 2 is the second KCL polymer mud on which we performed experiments. Following are the approach and parameters of the tests.

- Initial shear rate = 5 minutes
- Resting time = Varied for every test
- Linear shear rate = Varied in three different ways

We categorized linear shear rate in three different intervals. Then for one interval, we performed experiments by changing the resting time. Similarly, we continued for the other two intervals of the linear shear rate as well. For simplicity, we shall note down the results by making three cases.

5.2.1 Case Scenarios

Case A

0 to 2 per second in 0.5 seconds and maintained it for additional 30 seconds. This is the case mostly used by authors in literature.

Case B

0 to 5.1 per second in 0.5 seconds and maintained it for additional 30 seconds. This is a case which is similar to the field procedure. We wanted to examine maximum stress overshoot by going from 0 to 5.1 per second in the same time as in the case A of 0.5 seconds.

Case C

0 to 5.1 per second in 1.25 seconds and maintained it for additional 30 seconds. This time, we increased the time as well to reach from 0 to 5.1 per second in 1.25 seconds.

5.2.2 Case A

The following are the parameters of the tests performed.

- Initial shear rate = 5 minutes
- Resting time = Varied for every test
- Linear shear rate = 0 to 2 per second in 0.50 seconds

The results of maximum stress overshoot against varying times are shown in table 5.2 and figure 5.3.

WBM 2 – Case A	
Time (sec)	Max Stress overshoot (Pa)
20	3.902
30	4.031
60	4.378
120	4.725
300	4.889
600	5.038
1200	5.044
1800	5.23
3600	5.317
7200	5.899
10800	6.039
14400	5.834
18000	5.77

Table 5.2 Stress overshoots in the WBM 2 during 0 to 2 per second initial rate for 0.5 seconds following different resting times

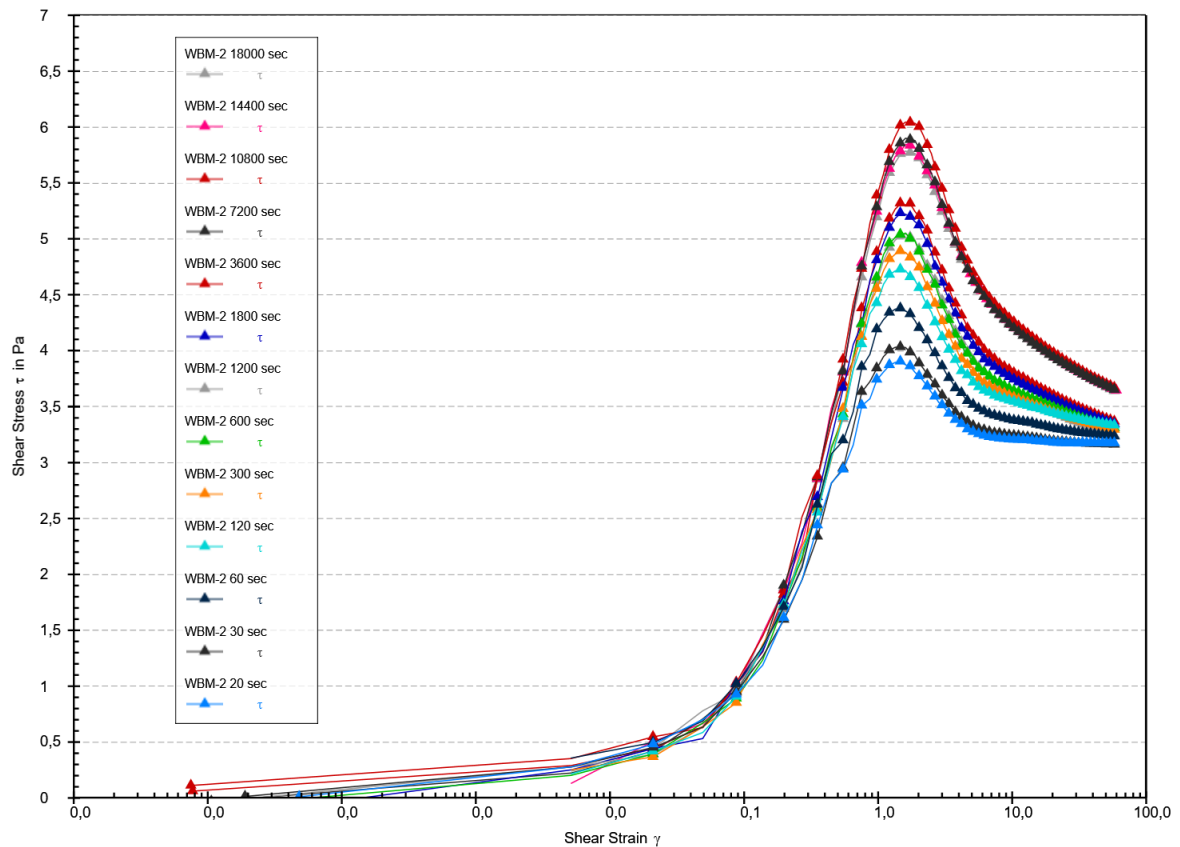


Figure 5.3 Stress overshoots in the WBM 2 during 0 to 2 per second initial rate for 0.5 seconds following different resting times

As seen from figure 5.3, initially by increasing the resting time, the value of maximum stress overshoot increased. This upward trend continued till 10800 seconds. However, for the

resting time of 14400 seconds, the value of maximum stress overshoot decreased from 6.039 Pa to 5.834 Pa. To confirm the trend, we performed another test for 18000 seconds. The value further decreased to 5.77 Pa yet quite close to 5.834 Pa. From this, we can deduce that for this particular mud and case, the maximum possible gel strength is 6.039 Pa. After this duration, no further gel strength would develop in the mud structure. This is possibly due to the settling of heavy particles in the mud system.

Furthermore, it can also be observed from figure 5.4, that for a longer period of resting time, the maximum value of stress overshoot deviates from the logarithmic trend. For instance, at resting time = 10800 seconds, the value is above the trend line. Subsequently, for resting time = 14400 seconds, the value is below the trendline.

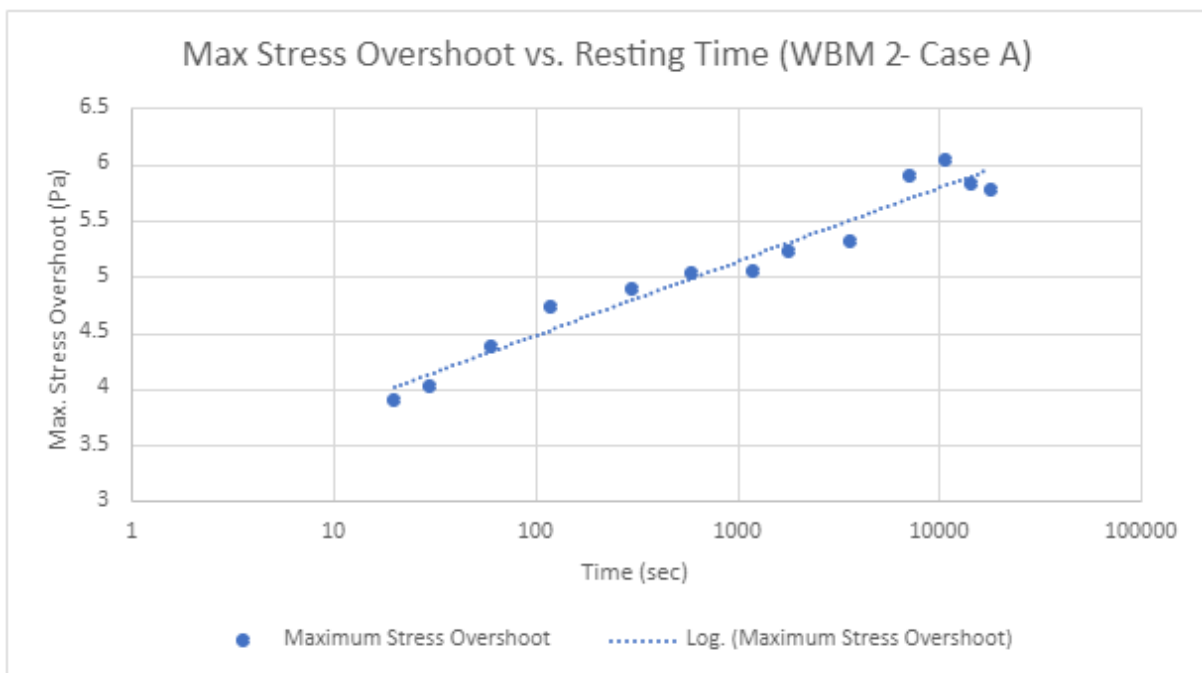


Figure 5.4 Maximum Stress overshoots in the WBM 2 as logarithmic function during 0 to 2 initial shear rate for 0.5 seconds following different resting times

5.2.3 Case B

The following are the parameters of the tests performed.

- Initial shear rate = 5 minutes
- Resting time = Varied for every test
- Linear shear rate = 0 to 5.1 per second in 0.5 seconds

The results of maximum stress overshoot against varying times are shown in table 5.3 and figure 5.5.

WBM 2 - Case B	
Time (sec)	Max Stress overshoot (Pa)
20	5.655
30	5.812
60	6.059
120	6.344
300	6.648
600	6.81
1200	7.221
1800	7.269
3600	7.427
7200	8.427
10800	8.441
14400	8.467
18000	8.828
21600	8.61

Table 5.3 Stress overshoots in the WBM 2 during 0 to 5.1 per second initial rate for 0.5 seconds following different resting times

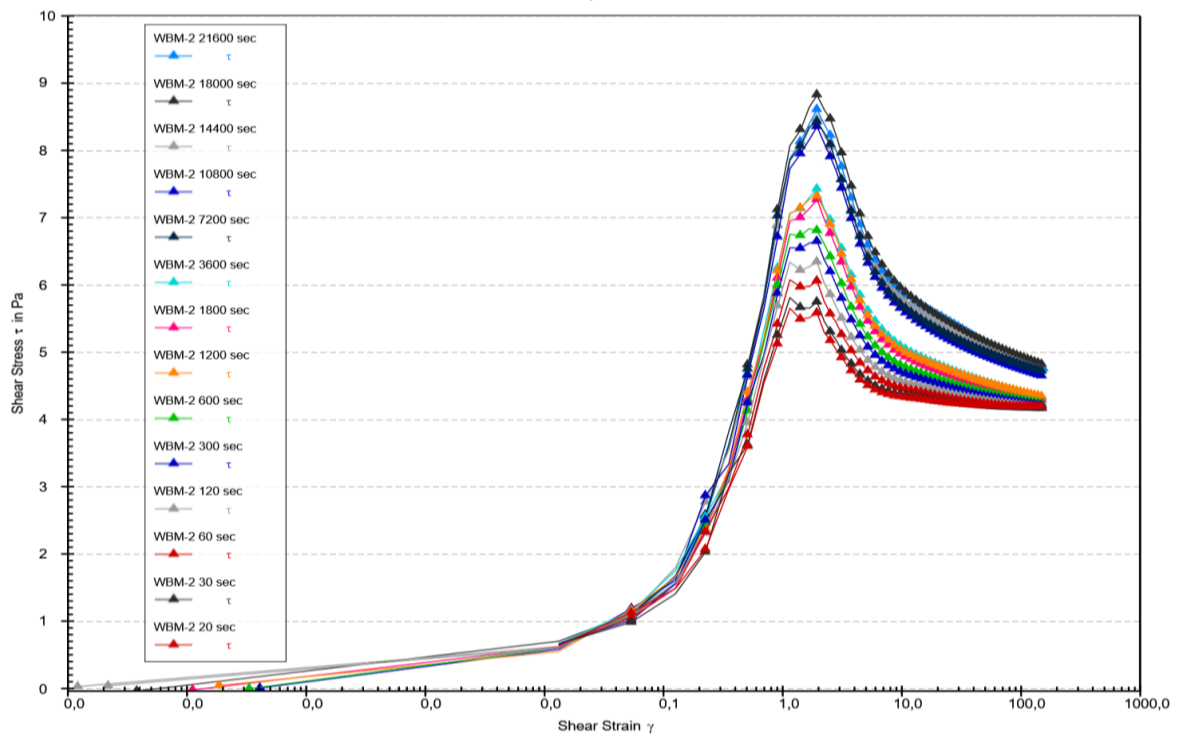


Figure 5.5 Stress overshoots in the WBM 2 during 0 to 5.1 per second initial rate for 0.5 seconds following different resting times

As evident from figure 5.5, the trend is similar to the trend observed in case A. In this particular case, 8.828 Pa can be considered maximum gel strength measured as maximum stress overshoot. It is very interesting to note that there exists a huge difference in the maximum value of gel strength between case A and case B. The values are 6.039 Pa and 8.828 respectively.

Furthermore, the trend of maximum stress overshoot vs. resting time is illustrated in figure 5.6. For a longer period of resting times, the values shift from the logarithmic trend.

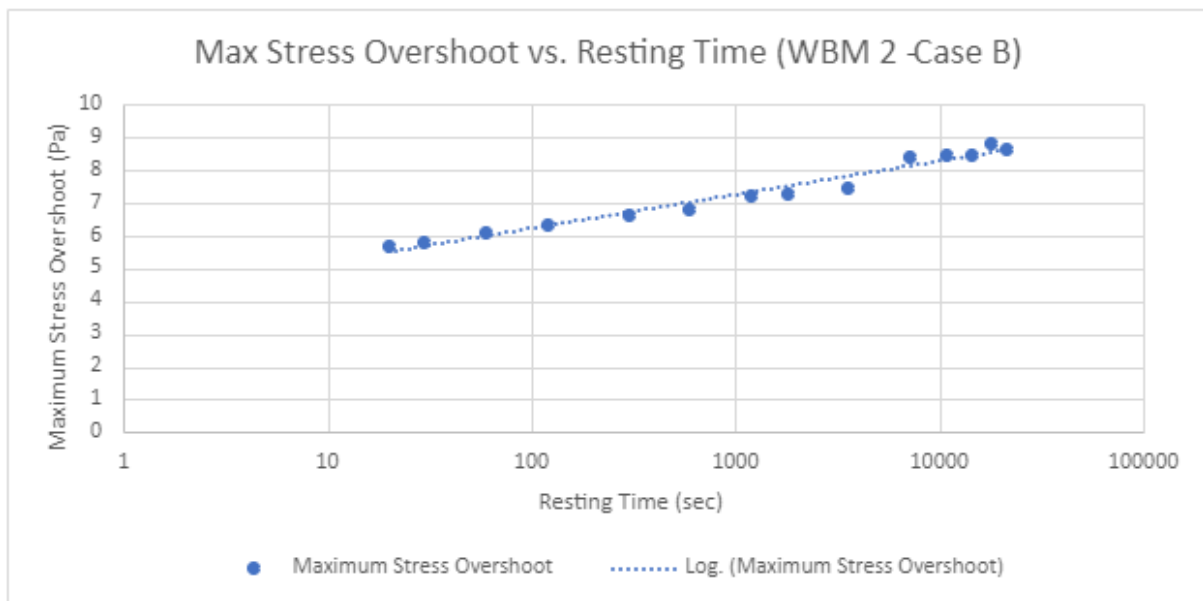


Figure 5.6 Maximum Stress overshoots in the WBM 2 as logarithmic function during 0 to 5.1 initial shear rate for 0.5 seconds following different resting times

5.2.4 Case C

The following are the parameters of the tests performed.

- Initial shear rate = 5 minutes
- Resting time = Varied for every test
- Linear shear rate = 0 to 5.1 per second in 1.25 seconds

The results of maximum stress overshoot against varying times are shown in table 5.4 and figure 5.7.

WBM 2 - Case C	
Time (sec)	Max Stress overshoot (Pa)
20	5.006
30	5.189
60	5.413
120	5.652
300	5.982
600	6.202
1200	6.869
1800	7.132
3600	7.153
7200	7.174
10800	7.301
14400	7.826
18000	7.648

Table 5.4 Stress overshoots in the WBM 2 during 0 to 5.1 per second initial rate for 1.25 seconds following different resting times

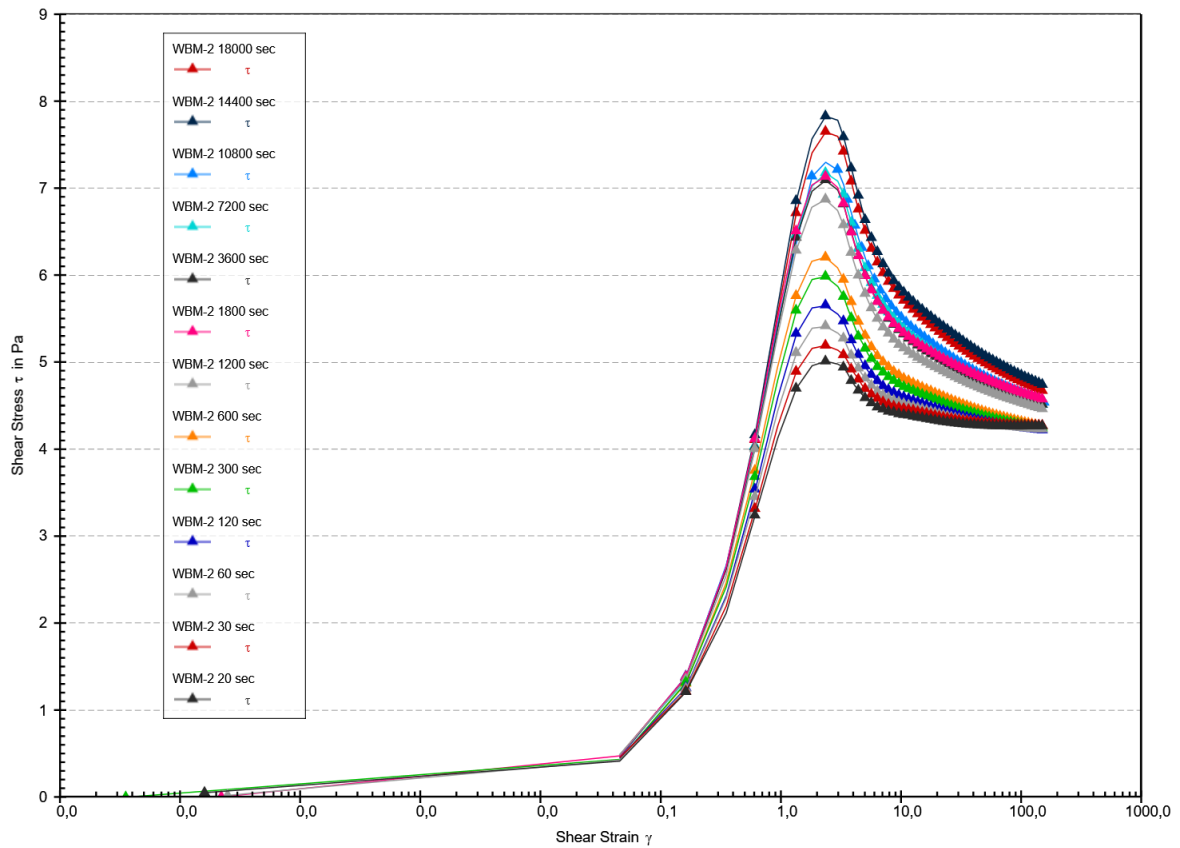


Figure 5.7 Stress overshoots in the WBM 2 during 0 to 5.1 per second initial rate for 1.25 seconds following different resting times

Figure 5.7 shows the trend which is similar to the previous cases. The difference lies in value though. The maximum value of stress overshoot, in this case, is reported as 7.826 Pa. Additionally, figure 5.8 shows the logarithmic trend between values of maximum stress overshoot and resting time.

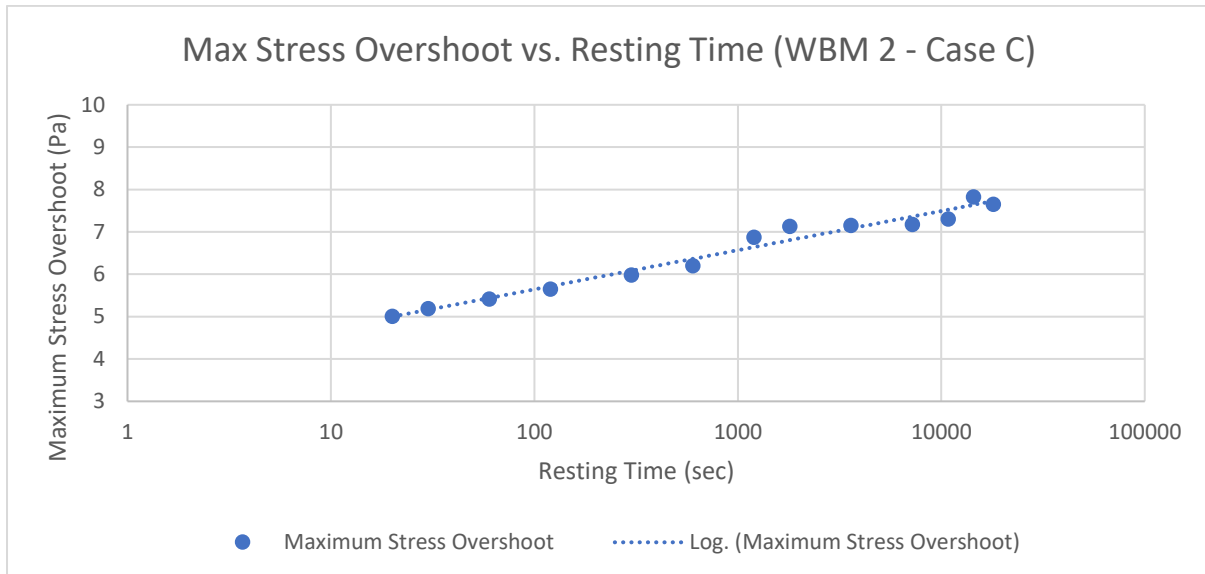


Figure 5.8 Maximum Stress overshoots in the WBM 2 as logarithmic function during 0 to 5.1 initial shear rate for 1.25 seconds following different resting times

Conclusion

For the given mud, the maximum value of stress overshoot continues to increase after 30 minutes. This trend continued for up to 5 hours (18000 seconds). The overall trend remained the same for all the cases. However, for case B, which is closer to the field practices, a significant increase in the stress overshoot values was observed. The maximum values for the three cases are 6.039 Pa, 8.828 Pa, and 7.826 Pa respectively. Additionally, for all three cases, there was a similar trend between maximum stress overshoot values and resting times as shown in figure 5.9.

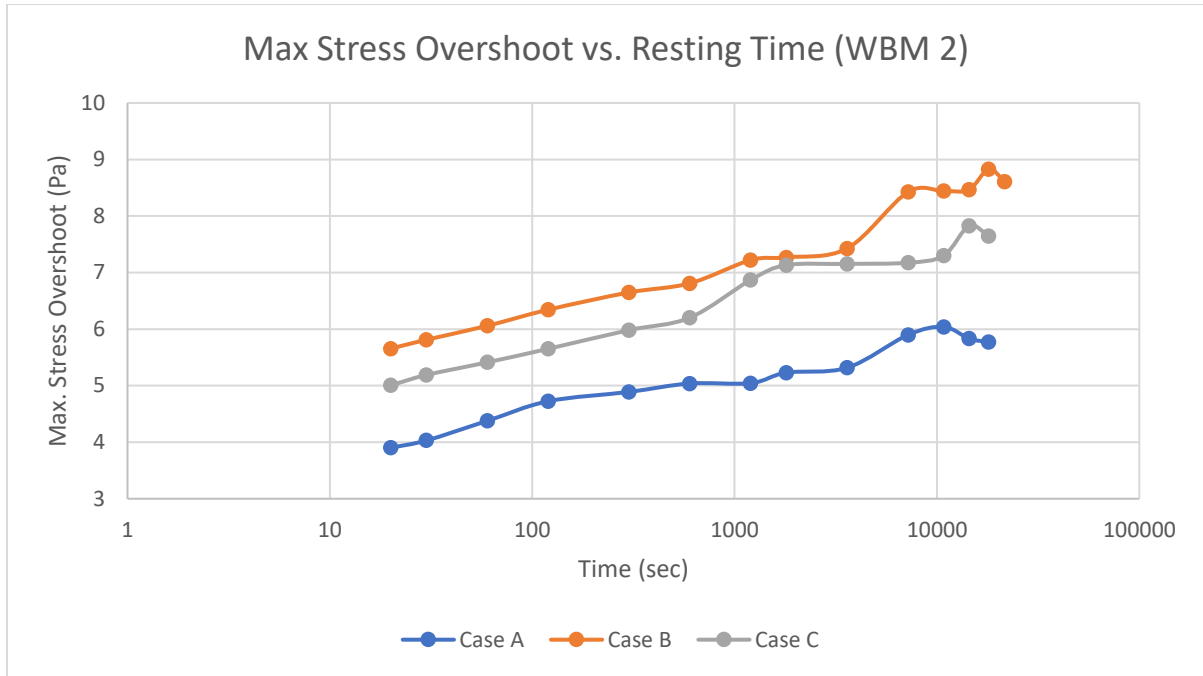


Figure 5.9 Comparison of case scenarios for WBM 2 following different resting times

5.3 ENVIROMUL OBM

Enviromul OBM is the third and the last mud on which we performed experiments. Following are the approach and parameters of the tests.

- Initial shear rate = 5 minutes
- Resting time = Varied for every test
- Linear shear rate = Varied in three different ways

Similar to WBM 2 testing, we categorized linear shear rate in three different intervals. Then for one interval, we performed experiments by changing the resting time. Similarly, we continued for the other two intervals of the linear shear rate as well. For simplicity, we shall note down the results by making three cases.

5.3.1 Case Scenarios

Case A

0 to 2 per second in 0.25 seconds and maintained it for additional 30 seconds. For the case of OBM, as compared to WBM, a relatively shorter shear rate ramp interval of 0.25 seconds was selected instead of 0.5 seconds. This was done to achieve the maximum value of shear stress

(2 per second) before the occurrence of maximum shear stress when the fluid begins to flow after the resting period [26]. This is the case mostly used by authors in literature.

Case B

0 to 5.1 per second in 0.25 seconds and maintained it for additional 30 seconds. This is a case which is similar to the field procedure. We wanted to examine maximum stress overshoot by going from 0 to 5.1 per second in the same time as in case A that is in 0.25 seconds.

Case C

0 to 5.1 per second in 0.625 seconds and maintained it for additional 30 seconds. This time, we increased the time as well to reach from 0 to 5.1 per second in 0.625 seconds.

5.3.2 Case A

The following are the parameters of the tests performed.

- Initial shear rate = 5 minutes
- Resting time = Varied for every test
- Linear shear rate = 0 to 2 per second in 0.25 seconds

The results of maximum stress overshoot against varying times are shown in table 5.5 and figure 5.10.

OBM - Case A	
Time (sec)	Max Stress overshoot (Pa)
20	6.026
30	6.27
60	6.825
120	7.299
300	7.833
600	8.378
1200	8.805
1800	9.118
3600	9.699
7200	9.39

Table 5.5 Stress overshoots in the Enviromul OBM during 0 to 2 per second initial rate for 0.25 seconds following different resting times

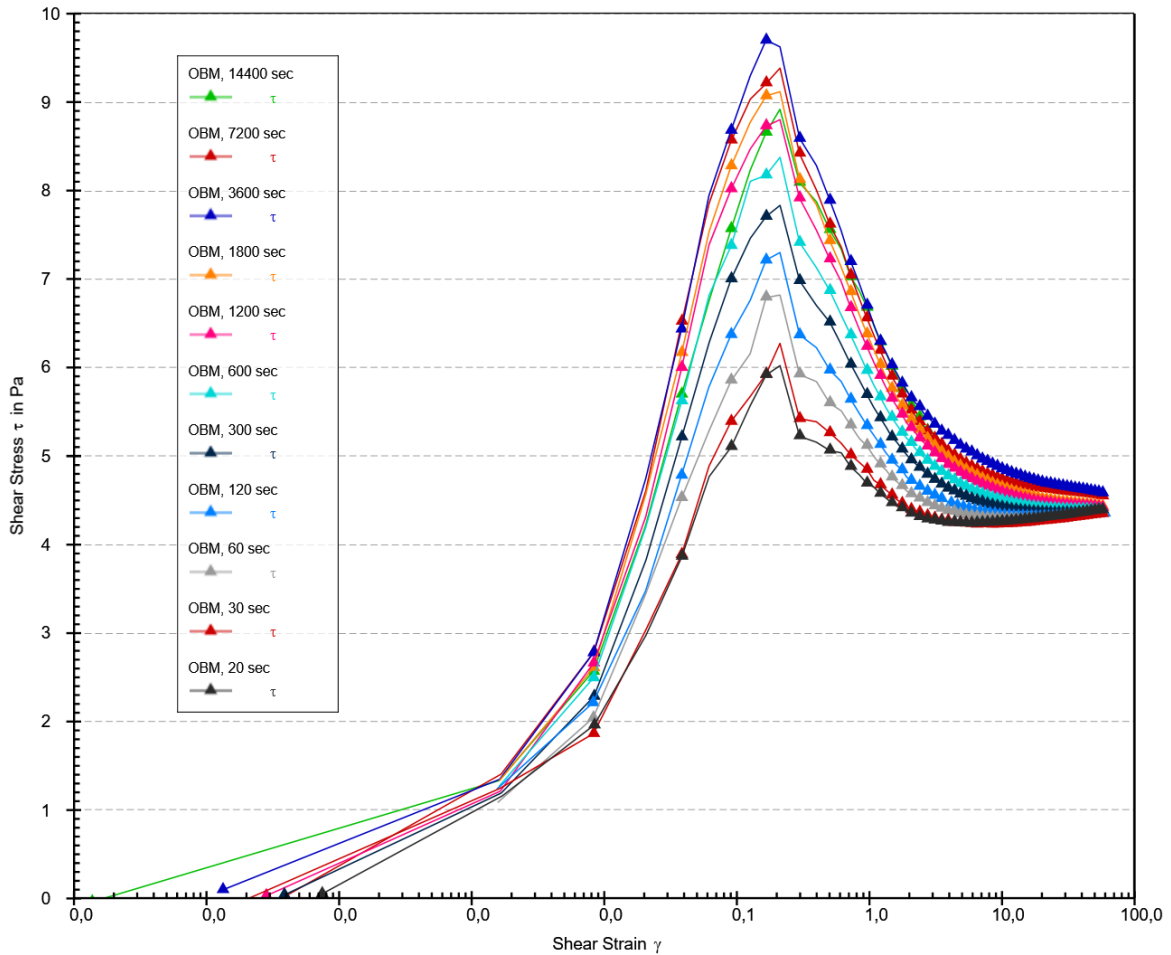


Figure 5.10 Stress overshoots in the Enviromul OBM during 0 to 2 per second initial rate for 0.25 seconds following different resting times

As seen from figure 5.10, initially by increasing the resting time, the value of maximum stress overshoot increased. This upward trend continued till 3600 seconds. However, for the resting time of 7200 seconds, the value of maximum stress overshoot decreased from 9.699 Pa to 9.39 Pa. This implies that for this particular OBM and case, the maximum possible gel strength is 9.699 Pa. After this duration, no further gel strength would develop in the mud structure. This is possibly due to the settling of heavy particles in the mud system.

Furthermore, it can also be observed from figure 5.11, that for a longer period of resting time, the maximum value of stress overshoot deviates from the logarithmic trend. For instance, at resting time = 1800 seconds, the value is above the trend line. Subsequently, for resting time = 7200 seconds, the value is below the trendline.

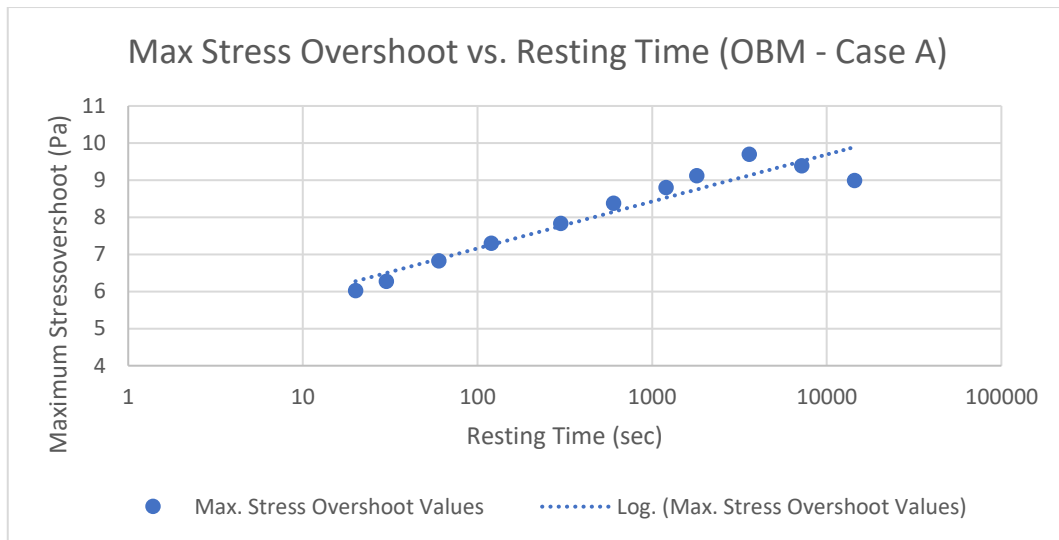


Figure 5.11 Maximum Stress overshoots in the Enviromul OBM as logarithmic function during 0 to 2 initial shear rate for 0.25 seconds following different resting times

5.3.3 Case B

The following are the parameters of the tests performed.

- Initial shear rate = 5 minutes
- Resting time = Varied for every test
- Linear shear rate = 0 to 5.1 per second in 0.25 seconds

The results of maximum stress overshoot against varying times are shown in table 5.6 and figure 5.12.

OBM - Case B	
Time (sec)	Max Stress overshoot (Pa)
20	8.995
30	8.947
60	9.361
120	9.795
300	10.545
600	11.034
1200	11.31
1800	12.387
3600	12.603
7200	12.344

Table 5.6 Stress overshoots in the Enviromul OBM during 0 to 5.1 per second initial rate for 0.25 seconds following different resting times

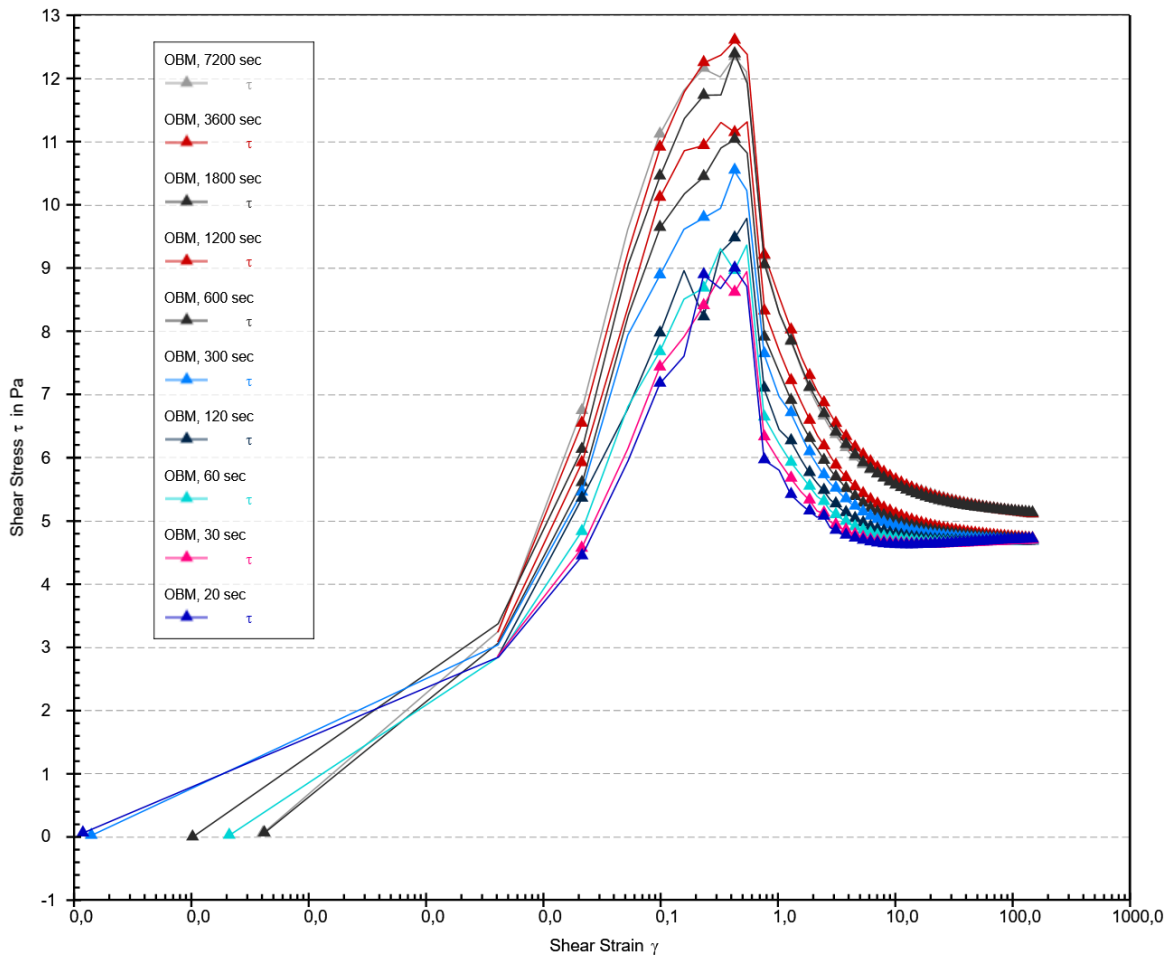


Figure 5.12 Stress overshoots in the Enviromul OBM during 0 to 5.1 per second initial rate for 0.25 seconds following different resting time

As it is clear from figure 5.12, the trend is similar to the trend observed in case A. In this particular case, 12.603 Pa can be considered gel strength measured as maximum stress overshoot. It is important to note that there exists a significant difference in the maximum value of gel strength between case A and case B. The values are 9.699 Pa and 12.603 Pa respectively.

Furthermore, the trend of maximum stress overshoot vs. resting time is illustrated in figure 5.13. For a longer period of resting times, the values shift from the logarithmic trend.

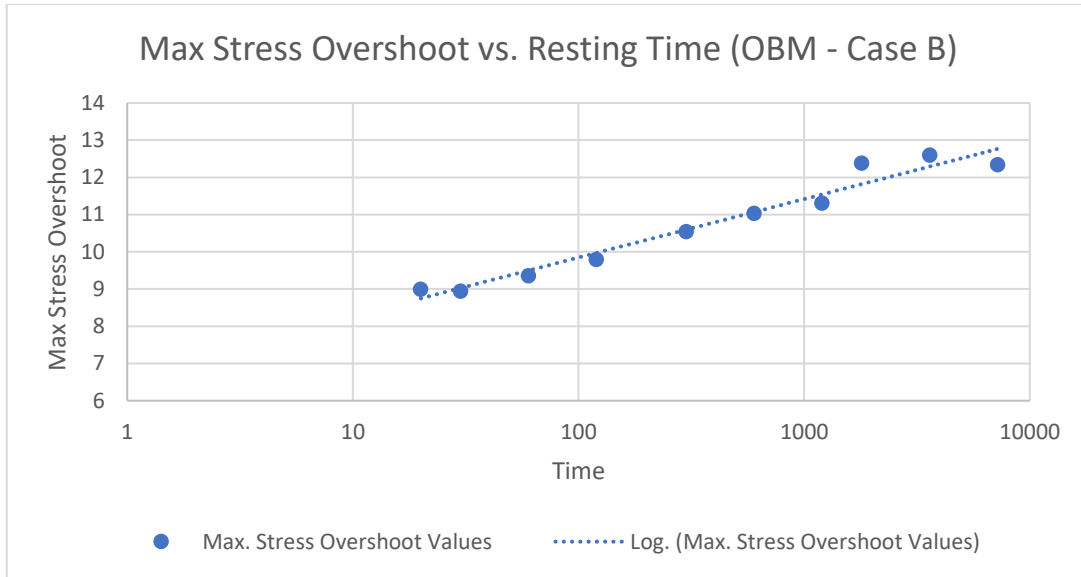


Figure 5.13 Maximum Stress overshoots in the Enviromul OBM as logarithmic function during 0 to 5.1 initial shear rate for 0.25 seconds following different resting times

5.3.4 Case C

The following are the parameters of the tests performed.

- Initial shear rate = 5 minutes
- Resting time = Varied for every test
- Linear shear rate = 0 to 5.1 per second in 0.625 seconds

The results of maximum stress overshoot against varying times are shown in table5.7 and figure 5.14.

OBM - Case C	
Time (sec)	Max Stress overshoot (Pa)
20	6.019
30	6.139
60	6.493
120	6.968
300	7.467
600	7.839
1200	8.327
1800	8.566
3600	8.822
7200	8.72

Table 5.7 Stress overshoots in the Enviromul OBM during 0 to 5.1 per second initial rate for 0.625 seconds following different resting times

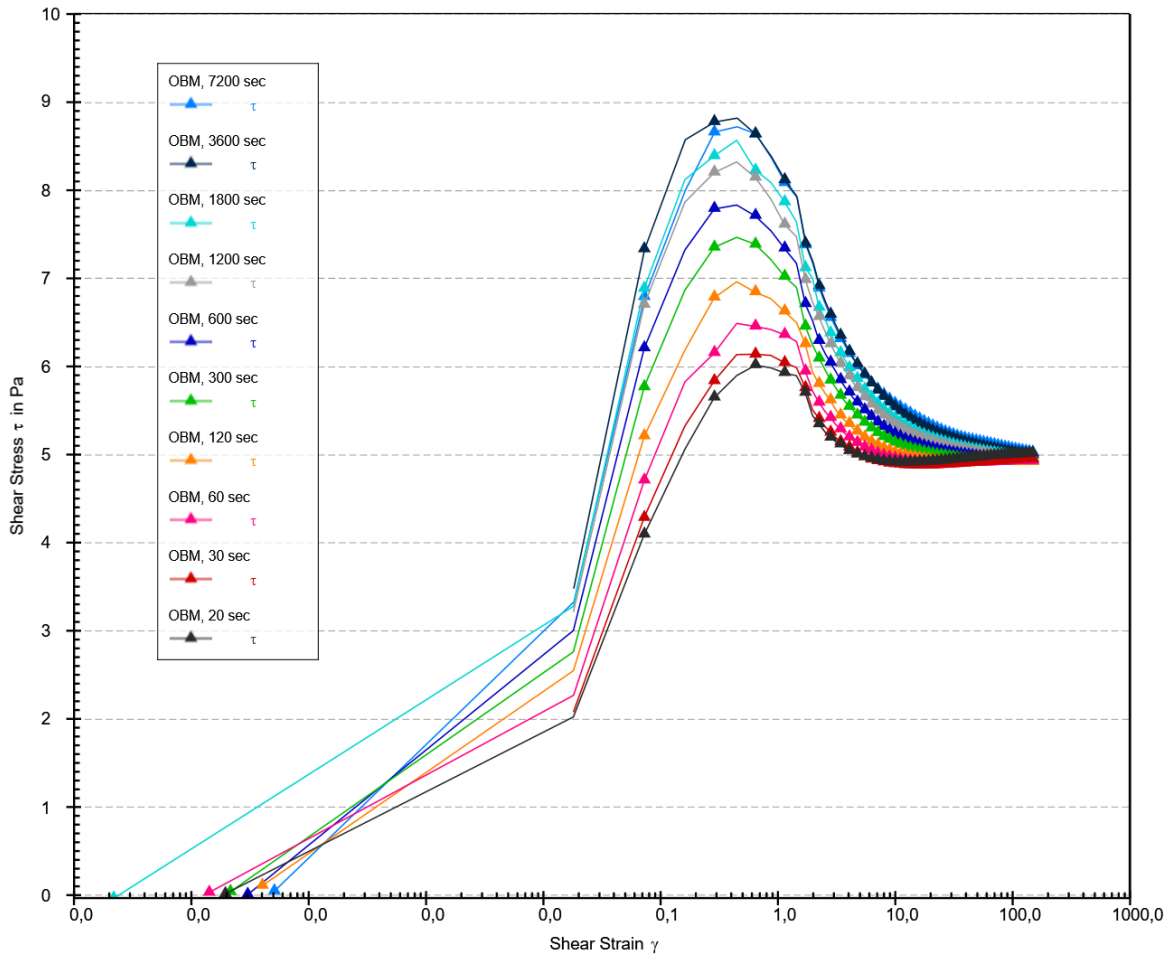


Figure 5.14 Stress overshoots in the Enviromul OBM during 0 to 5.1 per second initial rate for 0.625 seconds following different resting times

Figure 5.14 shows the trend which is similar to the previous cases. Nevertheless, there is a difference in the maximum value of maximum stress overshoot. The value, in this case, is reported as 8.822 Pa. Additionally, fig 5.15 shows the logarithmic trend between values of maximum stress overshoot and resting time.

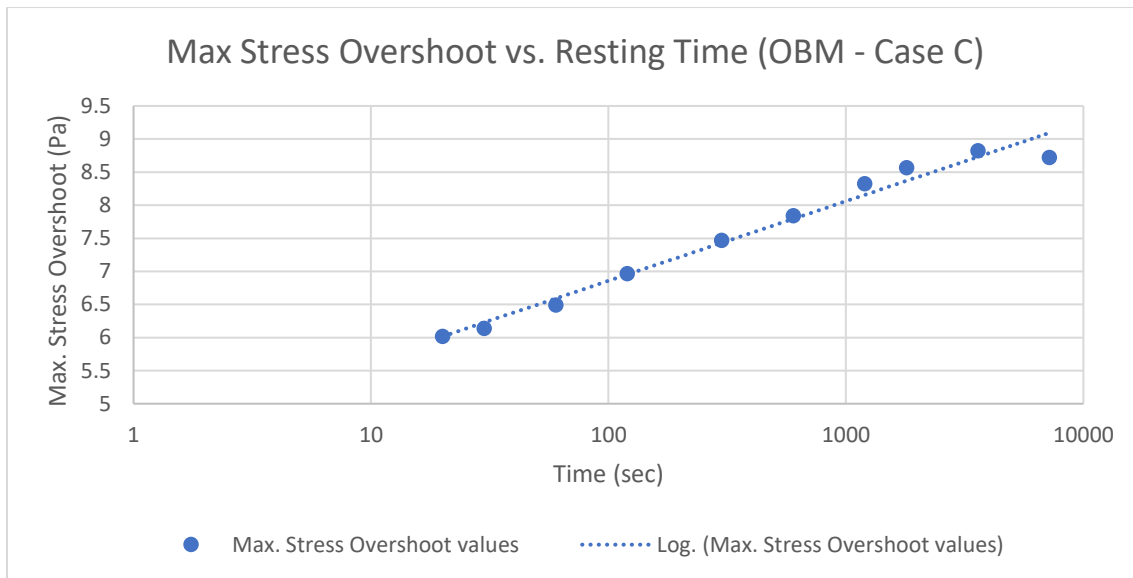


Figure 5.15 Maximum Stress overshoots in the Enviromul OBM as logarithmic function during 0 to 5.1 initial shear rate for 0.625 seconds following different resting times

Conclusion

For the given mud, the maximum value of stress overshoot continues to increase after 30 minutes. This trend continued for up to 1 hour (3600 seconds). The overall trend remained the same for all the cases. However, for case B, which is closer to the field practices, a significant increase in the stress overshoot values was observed. The maximum values for the three cases are 9.699 Pa, 12.603 Pa, and 8.822 Pa. Additionally, for all three cases, there was a similar trend between maximum stress overshoot values and resting times as shown in figure 5.16.

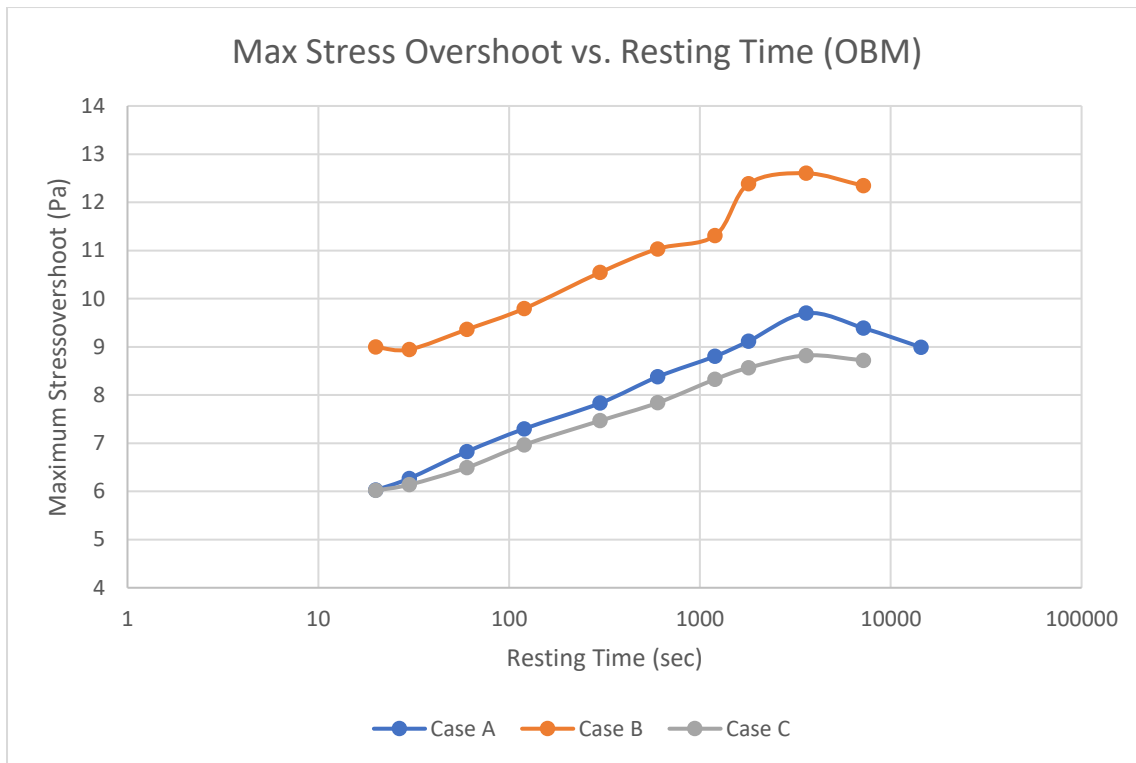


Figure 5.16 Comparison of case scenarios for Enviromul OBM following different resting times

5.4 Further Work Recommendations

Thixotropy and understanding gel strength is a complex mechanism. Within the stipulated time, we have tried to encapsulate the impact of various parameters on gel strength. However, there remain numerous possible areas of improvement and future research on the topic.

Firstly, the tests can be performed by using the rheometer and closing the lid of the sample bottle. This could have led to less vaporization and less sample drying effects, especially where the tests are run for longer durations. Secondly, another future improvement of this work could also include extending this work on various samples of water-based muds and oil-based drilling fluids. Performing the tests on different drilling fluid samples would increase the basis for comparison. Tests results at higher resting times could also be used to improve existing thixotropy models or to create a new model. Thirdly, the matrix of the testing could be extended by performing the tests at higher temperatures to simulate the temperature of the wellbore.

References

- [1] Lake, L.W. and L.W.M.R.F. Lake, *Petroleum Engineering Handbook, Volume 2 : Drilling Engineering*. 2006, Richardson: Richardson, US: Society of Petroleum Engineers.
- [2] Caenn, R., H.C.H. Darley, and G.R. Gray, *Composition and properties of drilling and completion fluids*. 2017, Gulf Professional Publishing.
- [3] Hughes, B., *Drilling Fluids Reference Manual*. Houston, Texas, 2006.
- [4] Alf Kristian Gjerstad, 2014. *Simplified Flow Equations for Single-Phase non-Newtonian Fluids in Couette-Poiseuille Flow and in Pipes*. PhD Thesis. UiS.
- [5] Radin Cedomir, 2013. *Main Pump Start-up Pressure Limitation Control System when using Thixotropic Drilling Fluids*. MSc Thesis. UiS.
- [6] Gofran Jafr, 2018. *Study of the mixing zone between two drilling fluids with large density difference, when using the Heavy Over Light (HOL) solution for terrestrial drilling*. MSc Thesis. UiS.
- [7] L.L.C., M.-I., *Drilling Fluids Engineering Manual*. 1998: M-I L.L.C.
- [8] Power, D. and M. Zamora. *Drilling fluid yield stress: measurement techniques for improved understanding of critical drilling fluid parameters*. in *National Technology Conference "Practical Solutions for Drilling Challenges": American Association of Drilling Engineers, Technical Conference papers, AADE-03-NTCE-35*. 2003.
- [9] Tanner, R.I., *Engineering rheology*. 2nd ed. ed. Oxford engineering science series. Vol. 52. 2000, Oxford: Oxford University Press.
- [10] Caenn, R., H.C.H. Darley, and G.R. Gray, *Composition and properties of drilling and completion fluids*. 2017, Gulf Professional Publishing.
- [11] Scott, P.D., M. Zamora, and C. Aldea. *Barite-sag management: challenges, strategies, opportunities*. in *IADC/SPE Drilling Conference*. 2004. Society of Petroleum Engineers.

- [12] Ida Sandvold, 2012. *Gel Evolution in Oil Based Drilling Fluids*. MSc thesis. NTNU
- [13] Hodne, H., *Drilling Fluid Technology , PET 210, The Laboratory compendium*, E.a. Petroleumtechnology, Editor. 2014. p. 122.
- [14] Chilingarian, G.V. and P. Vorabutr, *Drilling and drilling fluids*. Updated textbook ed. ed. Developments in petroleum science. Vol. 11. 1983, Amsterdam: Elsevier.
- [15] Bloys, B., et al., *Designing and managing drilling fluid*. Oilfield Review, 1994. 6(2): p. 33-43.
- [16] Fink, J.K., *Oil Field Chemicals, Fluid Loss Additives*. 2003: Elsevier Inc. 1-33.
- [17] Nguyen, T., et al., *Experimental study of dynamic barite sag in oil-based drilling fluids using a modified rotational viscometer and a flow loop*. Journal of Petroleum Science and Engineering, 2011. 78(1): p. 160-165.
- [18] Bern, P.A., et al., *Barite sag: Measurement, modeling, and management*. 2000. p. 25-30.
- [19] Hanson, P., et al. *Investigation of barite" sag" in weighted drilling fluids in highly deviated wells*. in *SPE Annual Technical Conference and Exhibition*. 1990. Society of Petroleum Engineers.
- [20] Ryen Caennl., et al., *The Rheology of Drilling Fluids*. 2017. Seventh edition.
- [21] Bjørkevoll K. S., Rommetveit R., Aas B., Gjeraldstveit H., Merlo A., *Transient gel breaking model for critical wells applications with field data*, in: SPE/IADC Drilling Conference, 19-21 February, Amsterdam, Netherlands, Society of Petroleum Engineers, 2003, pp. 1–8, SPE/IADC 79843.
- [22] Maxey, J., *Thixotropy and Yield Stress Behavior in Drilling Fluids*, in: AADE National Technical Conference and Exhibition, Houston, Texas, April 10-12, 2007, American Association of Drilling Engineers, 2007, pp. 1-10, AADE-07-NTCE-37.

- [23] Herzhaft B., Ragouilliaux A., Coussot P., *How To Unify Low- Shear-Rate Rheology and Gel Properties of Drilling Muds: A Transient Rheological and Structural Model for Complex Wells Applications*, in: IADC/SPE Drilling Conference, 21-23 February, Miami, Florida, USA, 2006, pp. 1–9, IADC/SPE 99080.
- [24] Ragouilliaux A., Herzhaft B., Bertrand F., Coussot P., *Flowin- stability and shear localization in a drilling mud*, *Rheol Acta*, 2006, 46, 261–271.
- [25] Cayeux E., Leulseged A., *Modelling of Drilling Fluid Thixotropy*, in: Proceedings of the ASME 2018 37th International Conference on Ocean,Offshore and Arctic Engineering, 2018, pp. 1–14, OMAE 2018-77203.
- [26] Hans Joakim Skadsem., Amare Leulseged., Eric Cayeux., *Measurement of Drilling Fluid Rheology and Modeling of Thixotropic Behavior*, in *Appl. Rheol*, 2019.
- [27] Barnes, H. A. (1996) “Thixotropy-a review”, *J. Non-Newtonian Fluid Mech.*, **70**, 1-33
- [28] Omland, T.H., *Particle settling in non-newtonian drilling fluids*. 2009.